HHS Public Access

Author manuscript

Mol Psychiatry. Author manuscript; available in PMC 2022 January 16.

Published in final edited form as:

Mol Psychiatry. 2021 November ; 26(11): 6704–6722. doi:10.1038/s41380-021-01093-2.

Pharmacological and behavioral divergence of ketamine enantiomers: implications for abuse liability

Jordi Bonaventura[1,*], **Sherry Lam**[1], **Meghan Carlton**[1], **Matthew Boehm**[1], **Juan L. Gomez**[1], **Oscar Solís**[1], **Marta Sánchez-Soto**[2], **Patrick J. Morris**[3], **Ida Fredriksson**[4], **Craig J. Thomas**[3], **David R. Sibley**[2], **Yavin Shaham**[4], **Carlos A. Zarate Jr**[5], **Michael Michaelides**[1,6,*]

[1]Biobehavioral Imaging and Molecular Neuropsychopharmacology Unit, National Institute on Drug Abuse Intramural Research Program, Baltimore, MD, 21224

[2]Molecular Neuropharmacology Section, National Institute of Neurological Disorders and Stroke Intramural Research Program, Bethesda, MD, 20892

[3]Division of Preclinical Innovation, National Center for Advancing Translational Sciences, Rockville, MD, 20850

[4]Neurobiology of Relapse Section, National Institute on Drug Abuse Intramural Research Program, Baltimore, MD, 212245

[5]Experimental Therapeutics and Pathophysiology Branch, National Institute of Mental Health, Intramural Research Program, Bethesda, MD, 20892

[6]Department of Psychiatry and Behavioral Sciences, Johns Hopkins Medicine, Baltimore, MD, 21205

Abstract

Ketamine, a racemic mixture of (S)-ketamine and (R)-ketamine enantiomers, has been used as an anesthetic, analgesic and more recently, as an antidepressant. However, ketamine has known abuse liability (the tendency of a drug to be used in non-medical situations due to its psychoactive effects), which raises concerns for its therapeutic use. (S)-ketamine was recently approved by the United States' FDA for treatment-resistant depression. Recent studies showed that (R)-ketamine has greater efficacy than (S)-ketamine in preclinical models of depression, but its clinical antidepressant efficacy has not been established. The behavioral effects of racemic ketamine have been studied extensively in preclinical models predictive of abuse liability in humans (self-administration and conditioned place preference [CPP]). In contrast, the behavioral effects of each enantiomer in these models are unknown. We show here that in the intravenous

*Correspondence: jordi.bonaventura@nih.gov, mike.michaelides@nih.gov.

Contributions

All authors critically reviewed the content and approved the final version before submission. J.B., S.L., M.C., M.B., J.L.G., O.S-C and M.S-S performed the experiments. J.B., S.L., M.S-S., I.F. and M.M. analyzed the data. J.B., I.F., Y.S. and M.M. supervised experiments. P.J.M, C.J.T., D.R.S., C.A.Z, provided access to resources and support. J.B. and M.M. designed the study and wrote the manuscript with input from all coauthors.

Conflict of interest

All other authors declare no conflict of interest.

drug self-administration model, the gold standard procedure to assess potential abuse liability of drugs in humans, rats self-administered (S)-ketamine but not (R)-ketamine. Subanesthetic, antidepressant-like doses of (S)-ketamine, but not of (R)-ketamine, induced locomotor activity (in an opioid receptor-dependent manner), induced psychomotor sensitization, induced CPP in mice, and selectively increased metabolic activity and dopamine tone in medial prefrontal cortex (mPFC) of rats. Pharmacological screening across thousands of human proteins and at biological targets known to interact with ketamine yielded divergent binding and functional enantiomer profiles, including selective mu and kappa opioid receptor activation by (S)-ketamine in mPFC. Our results demonstrate divergence in the pharmacological, functional, and behavioral effects of ketamine enantiomers, and suggest that racemic ketamine's abuse liability in humans is primarily due to the pharmacological effects of its (S)-enantiomer.

Keywords

Biological Sciences/Pharmacology; ketamine abuse depression

Introduction

Ketamine, a racemic mixture of (S)-ketamine and (R)-ketamine enantiomers, is a widely used analgesic and dissociative anesthetic [1]. Subanesthetic doses of ketamine produce rapid antidepressant effects in individuals with major depressive disorder (MDD), bipolar depression, and treatment-resistant depression (TRD) [2–9]. Nevertheless, ketamine is a controlled substance, has known abuse potential (the tendency of a drug to be used in non-medical situations due to its psychoactive effects [9]), and can induce undesirable side effects [11,12].

(S)-ketamine (esketamine, Spravato®) recently received "Fast Track" and "Breakthrough Therapy" designation and approval by the FDA as an intranasal formulation for TRD and MDD with acute suicidal ideation or behavior [13, 14]. However, this approval was not without controversy as (S)-ketamine's efficacy and abuse liability are a concern [15, 16]. Furthermore, in rodents, (R)-ketamine shows greater antidepressant-like efficacy and less psychotomimetic effects than (S)-ketamine [17]. In humans, a recent open-label study with (R)-ketamine showed antidepressant efficacy without dissociative effects [18]. However, placebo controlled double-blind clinical trials are needed to confirm this finding.

Ketamine is generally regarded as a non-competitive N-methyl-D-aspartate receptor (NMDAR) antagonist, with the allosteric phencyclidine (PCP) binding site in the NMDAR considered ketamine's primary target [19, 20]. However, ketamine's affinity for NMDARs is in the micromolar range [19–22] and its selectivity for NMDARs over other known or unidentified receptors and cellular targets is a subject of debate [20]. Indeed, ketamine shows affinity for both opioid and sigma receptors [21–23] and produces changes in dopamine signaling [24–26]. Therefore, it is unclear how the complex pharmacological profile of ketamine (for review see [19]) relates to its therapeutic effects and abuse liability profile.

Several studies investigated racemic ketamine pharmacology and potential abuse liability, as assessed in the drug self-administration procedure in rats and monkeys [27–31]. The drug self-administration model in these species has been used since the 1960s by both academic researchers and the pharmaceutical industry to predict the abuse liability of psychoactive drugs [32]. However, no study to date has characterized (S)-ketamine and (R)-ketamine self-administration and very few studies characterized other *in vivo* and *in vitro* pharmacological properties of its enantiomers [17,19].

(S)-ketamine is approved and (R)-ketamine is currently being investigated for the treatment of depression [2–9]. Depression is often comorbid with substance use disorders [33]. Therefore, in the present study we first pharmacologically characterized ketamine's (S)- and (R)- enantiomers. Next, we assessed the behavioral effects of (S)-ketamine and (R)-ketamine in three standard behavioral procedures commonly used to assess the behavioral effects of drugs that are voluntarily consumed by humans or used when they are no longer medically needed or without prescription: locomotor sensitization, conditioned place preference [CPP], and intravenous drug self-administration [34–36].

Results

(S)-ketamine and (R)-ketamine show divergent *in vitro* target engagement profiles and weak NMDAR selectivity

Ketamine and its enantiomers are generally regarded as competitive NMDAR antagonists, but these compounds have also been reported to interact with other receptors and proteins [19–26]. To obtain a greater understanding on the binding profile of each enantiomer, we first screened each enantiomer for competitive binding or inhibition against a selected panel of 98 receptors and enzymes, including known targets for addictive drugs and medications (Figure 1A). We did not identify any 'hits' (defined as >50% inhibition of binding to a given receptor or enzyme) when we used 100 nM of each enantiomer as a screening concentration (Figure 1A). At 10 μM, the PCP binding site of the NMDAR was identified as a positive hit for both (S)-ketamine and (R)-ketamine. At this same concentration, the mu-opioid receptor (MOR) was identified as a hit for (S)-ketamine but not for (R)-ketamine (Figure 1A). No other hits were identified at this dose.

To confirm these findings and extend them to measurements of the affinity of the enantiomers for each receptor, we tested (S)- and (R)-ketamine using competitive radioligand binding assays in rat whole brain tissue. (S)-ketamine showed a ~5-fold higher affinity for NMDAR (Ki=0.8 ± 0.2 μM) compared to (R)-ketamine (Ki: 5 ± 2 μM) (Figure 1B). (S)-ketamine also bound with higher affinity (Ki: 7 ± 3 μM) than (R)-ketamine (Ki: 19 ± 5 μM) to MORs. Though the screen did not identify KORs as a valid hit, 10 μM (S)-ketamine did produce ~35% inhibition of KOR binding, whereas 10 μM (R)-ketamine had a much weaker effect (~13% inhibition). We also measured the affinity for (S)-ketamine (Ki: 14 ± 7 μM) and (R)-ketamine (40 ± 10 μM) at KORs (Figure 1C). Finally, sigma (σ) binding sites share homology with opioid binding sites and have been implicated in the actions of ketamine [19, 21–23]. However, these binding sites were not included in the aforementioned screen. In contrast to the greater affinity of (S)-ketamine at NMDAR, MOR, and KOR, (R)-ketamine (Ki=27 ± 3 μM) showed greater affinity than (S)-ketamine (131 ±

15 μM) for sigma-1 (σ_1), and sigma-2 (σ_2) 'receptors' (Ki=0.5 ± 0.1 mM and 2.8 ± 0.7 mM, respectively) (Figure 1D).

The above results show that the selectivity of either enantiomer for NMDARs over opioid receptors is between 5 to 20-fold. This is a small difference as the canonical, high affinity NMDAR antagonist MK-801 shows ~1000-fold selectivity for NMDAR over opioid receptors. Furthermore, whereas ketamine enantiomers are known non-competitive antagonists at NMDARs [19,20], their mode of action at MOR and KOR is not well established [19, 21, 23]. We reasoned that the small selectivity window between NMDARs, MORs, and KORs could be of even lower significance if ketamine activated opioid receptors.

To examine this question, we measured the ability of (S)- and (R)-ketamine to activate different MOR and KOR signaling pathways. Opioid receptor activation leads to inhibition of cyclic adenosine monophosphate (cAMP) accumulation and/or recruitment of ß-arrestin-triggered signaling pathways. We found that in the cAMP assay, (S)-ketamine behaved as a partial agonist at MOR and as a full agonist at KOR (Figure 1E), (MOR: EC_{50} = 9 ± 2 μM, E_{max} = 48 ± 3 %; KOR: EC_{50} = 16 ± 4 μM, E_{max} = 84 ± 5 %). (R)-ketamine was a weaker partial agonist at both receptors (MOR: EC_{50} = 34 ± 14 μM, E_{max} = 39 ± 3 %; KOR: EC_{50} > 100 μM, E_{max} < 50 %). Neither (S)- nor (R)-ketamine activated the ß-arrestin pathway (Figure 1F). Finally, and consistent with their micromolar binding affinities, neither enantiomer antagonized or modulated morphine signaling at concentrations below 1 μM (the concentration at which they start activating the receptor on their own (Figure 1G)).

In summary, these findings indicate that (S)- and (R)-ketamine exhibit divergent *in vitro* target engagement and functional profiles, which along with NMDARs, also include MOR, KOR, and sigma receptors. Specifically, we found that both enantiomers bound to NMDARs, with (S)-ketamine showing higher affinity that (R)-ketamine. Similarly, both enantiomers bound to and activated MORs and KORs, with (S)-ketamine showing higher affinity and potency than (R)-ketamine. In contrast, we found that (R)-ketamine bound to sigma-1 and sigma-2 receptors with higher affinity than (S)-ketamine.

(S)-ketamine and (R)-ketamine exhibit divergent pharmacokinetics and negligible off-target profiles

To obtain insight into the *in vivo* target engagement profile of each enantiomer, we radiolabeled (S)- and (R)-ketamine with ^{11}C and performed positron emission tomography (PET) in rats. Prior studies conducted in both laboratory animals and in humans showed mixed results in their attempt to visualize NMDAR density using [^{11}C]ketamine and PET [37–39], indicating that ketamine is not a reliable tracer for PET imaging of NMDARs [37]. This is expected, given ketamine's low affinity at the NMDAR. Instead, our goal was to use PET to examine potential differences in brain uptake, clearance, and distribution between [^{11}C](S)- and [^{11}C](R)-ketamine synthesized at higher specific activity than in prior studies [37–39]. Our second goal was to rule out the existence of NMDAR-independent high-affinity interactions in the rat brain.

In agreement with prior studies [37–39], PET imaging with intravenous (IV) [^{11}C](S)- and [^{11}C](R)-ketamine revealed rapid brain uptake and fast clearance of each enantiomer, indicating that these compounds lack high affinity targets in the rat brain (Figures 2A to 2D). [^{3}H]MK-801 exhibits high affinity and has been used to measure NMDAR binding [35]. Our in vitro binding data, and data from other studies indicate that ketamine fully displaces [^{3}H]MK-801 binding to NMDARs, both *in vitro* and *in vivo* [40]. However, the low affinity of the radiolabeled enantiomers would make them unsuitable to label NMDARs using PET. We found that the *in vivo* brain uptake of [^{11}C](S)- and [^{11}C](R)-ketamine was not inhibited after pretreatment with a standard pharmacological and behaviorally effective dose of MK-801 (1 mg/kg, IP) (Figure 2B and D). This observation confirms that these radiolabeled enantiomers do not exhibit sufficient affinity to label NMDARs using PET. However, [^{11}C](S)- and [^{11}C](R)-ketamine uptake was also not affected after pretreatment of pharmacological doses of non-radiolabeled enantiomers, indicating that the brain uptake was non-specific. In sum, these PET studies show that [^{11}C](S)- and [^{11}C](R)-ketamine brain uptake in the rat is neither NMDAR-dependent nor indicative of high affinity binding to other targets.

In vivo binding of [^{11}C](S)- and [^{11}C](R)-ketamine to NMDARs might be activity-dependent [41]. Therefore, we synthesized and then injected (IV) [^{3}H](S)-ketamine or [^{3}H](R)-ketamine to awake rats and collected their brains and peripheral organs at different time points. In agreement with the results from our *in vivo* PET studies, *ex vivo* autoradiographic analysis of brain sections from rats that received IV injections of either [^{3}H](S)- or [^{3}H](R)-ketamine did not show any brain regional enrichment. Furthermore, and consistent with the *in vivo* PET results, the observed brain distribution of [^{3}H](S)- or [^{3}H](R)-ketamine was not blocked, either by pretreatment with MK-801 (1 mg/kg, IP) or non-radiolabeled ketamine (10 or 65 mg/kg, IP) (Supplemental Figure 1). [^{3}H](R)-ketamine showed higher brain uptake compared to [^{3}H](S)-ketamine (Figure 2E). This observation also coincided with lower levels of [^{3}H](R)-ketamine compared to [^{3}H](S)-ketamine in the liver and kidneys (Figure 2F), indicative of slower metabolization of (R)-ketamine [42]. In sum, like our *in vivo* PET findings, these *ex vivo* results show that [^{3}H](S)- and [^{3}H](R)-ketamine exhibit non-specific brain uptake and lack of high-affinity binding. Our *ex vivo* results also indicate that anesthesia does not contribute to lack of NMDAR engagement, as observed in [^{11}C](S)- and [^{11}C](R)-ketamine PET studies (Figure 2A-F).

To further confirm the lack of high affinity specific binding sites for (S)- and (R)-ketamine in the rat brain, we examined the binding profile of [^{3}H](S)- and [^{3}H](R)-ketamine (tested up to 300 nM) by performing binding assays in whole brain homogenates of rats. We did not observe any displaceable or saturable [^{3}H](S)- and [^{3}H](R)-ketamine binding, indicating a lack of high affinity specific binding in both membrane and cytosolic fractions (Figures 2G and 2H).

Finally, to assess whether the [^{3}H](S)- and [^{3}H](R)-ketamine binding profile we observed in rats extends to humans, we tested [^{3}H](S)- and [^{3}H](R)-ketamine for binding to the high density HuProt™ (>16,000 human genes; ~81% of the human proteome) and Protoarray® microarrays (>9000 human proteins). We found that neither assay yielded any high affinity specific binding hits (Supplemental Figures 2–3). Notably, high density protein arrays can

be susceptible to improper protein folding, especially for membrane proteins. To address this issue, we leveraged Retrogenix™ target deconvolution technology to test [^{3}H](S)- and [^{3}H](R)-ketamine binding to >6000 cell surface and secreted human proteins transiently transfected in HEK-293 cells. Once again, no high affinity specific binding hits were found (Supplemental Figure 4).

In sum, our results from PET and *ex vivo* uptake experiments, along with our target deconvolution findings indicate that (S)- and (R)-ketamine lack high affinity binding targets and exhibit negligible off-target binding profiles (i.e., they do not bind with high affinity at biological targets other than those previously identified).

Different effect of (S)-ketamine and (R)-ketamine on metabolic activity, dopamine tone, and MOR-signaling

To profile *in vivo* effects of subanesthetic doses of (S)- and (R)-ketamine on regional brain activity, we used [^{18}F]fluorodeoxyglucose (FDG) assisted metabolic mapping and PET. Clinically, ketamine is administered IV over a period of ~40 min. Therefore, we chose a similar method of administration for our experiments. We administered a low, subanesthetic intravenous dose of (S)- or (R)-ketamine (10 mg/kg) over 40 min together with IP FDG injection to awake and freely behaving male rats. After the uptake period, we anesthetized the rats and scanned their brains using PET (Figure 3A). We found that (S)- and (R)-ketamine elicited distinct patterns of regional brain activity. Specifically, (S)-ketamine selectively increased activity in the medial prefrontal cortex (mPFC) (one-way ANOVA; $T(1,7)>1.89$, $p \leq 0.05$) whereas (R)-ketamine did not (Figures 3B and 3C). In contrast, (R)-ketamine selectively decreased in activity in the mediodorsal nuclei of the thalamus, including the paraventricular and habenular regions (one-way ANOVA; $T(1,7)>1.89$, $p \leq 0.05$) whereas (S)-ketamine did not (Figure 3C). Other brain areas showed similar metabolic activity in response to each enantiomer. For example, both enantiomers decreased activity in the superior colliculus (where MOR receptors are highly enriched) and increased activity in the lateral hippocampus (one-way ANOVA; $T(1,7)>1.89$, $p \leq 0.05$). Overall, these results recapitulate the effects of subanesthetic doses of racemic ketamine on brain metabolic activity reported in previous *ex vivo* [^{14}C]-2-deoxyglucose studies [43, 44]. More important, our results extend these prior findings by demonstrating the selective contribution of each enantiomer to discrete *in vivo* brain metabolic activity signatures.

In preclinical studies, the mPFC and opioid receptors play important roles in ketamine's preclinical antidepressant-like efficacy [45–48]. In humans, opioid receptors have been implicated in ketamine's antidepressant efficacy [49, 50] and hypothesized to underlie risks associated with its abuse liability in humans [16]. To confirm whether the selective effect of (S)-ketamine on mPFC metabolic activation coincides with selective effects on opioid receptor activity in this region, we performed [^{35}S]GTPγS autoradiography [51] assays in mPFC-containing rat brain sections (Figure 3D). We found that 10 μM (S)-ketamine, but not (R)-ketamine, induced significant (~50% the response of 1 μM morphine) [^{35}S]GTPγS recruitment in the mPFC (one way ANOVA, factor: treatment ($F(5, 55) = 12.7$, $p < 0.0001$), post-hoc tests: morphine (adjusted $p < 0.001$) and (S)-ketamine ($p = 0.001$)) (Figures 3E and 3F). The [^{35}S]GTPγS assay is mostly sensitive to inhibitory Gi/o coupled proteins

[51] and both MOR and KOR are expressed in the mPFC [52, 53]. We confirmed that the (S)-ketamine induced [^{35}S]GTPγS recruitment in the mPFC was due to opioid receptor activation: an opioid receptor antagonist naloxone (10 μM) prevented (S)-ketamine-induced [^{35}S]GTPγS recruitment (adjusted $p = 0.02$). As stated above, 10 μM (R)-ketamine failed to significantly increase [^{35}S]GTPγS recruitment and naloxone did not alter [^{35}S]GTPγS recruitment after (R)-ketamine exposure.

Excitatory projections from the mPFC play a key role in regulating the activity of dopaminergic neurons in the ventral tegmental area (VTA) [54] that are critical to the behavioral effects of drug and non-drug rewards [55]. In the experiments described above we showed that (S)-ketamine has greater NMDAR and MOR potency than (R)-ketamine. It is known that NMDAR, MOR, and KOR regulate VTA neuronal activity [53, 56–58] and a prior PET study in awake monkeys reported decreases in [^{11}C]raclopride binding (i.e., increased dopamine tone) in response to (S)-ketamine but not (R)-ketamine [59]. Therefore, we reasoned that (S)-ketamine would have greater effects than (R)-ketamine on dopaminergic activity. Like [^{11}C]raclopride, the *in vivo* uptake of the dopamine D2/D3 receptor PET radioligand [^{18}F]fallypride is sensitive to variations in extracellular dopamine concentrations [60]. Therefore, [^{18}F]fallypride displacement is used to infer pharmacologically-evoked regional changes in extracellular dopamine levels in the rodent and human brain [60]. Therefore, we examined the extent to which 10 mg/kg IV infusion of each ketamine enantiomer for 40 min would change regional [^{18}F]fallypride displacement and by extension, regional changes in *in vivo* dopamine tone (Figures 3G and 3H). Neither (S)- nor (R)-ketamine significantly changed global extracellular dopamine levels in the dorsal striatum (Figures 3I and 3J). In contrast, other midbrain dopamine projection sites such as mPFC, septum, and globus pallidus showed increased [^{18}F]fallypride displacement, (i.e., higher dopamine tone) in rats infused with (S)-ketamine, whereas somatosensory cortex and nucleus accumbens showed higher dopamine tone when rats were infused with (R)-ketamine (one-way ANOVA; $T(1,18)>1.73$, $p \leq 0.05$) (Figure 3K).

In sum, these results show that low, subanesthetic IV doses of (S)- or (R)-ketamine lead to divergent regional changes in both brain metabolic activity and dopamine tone. More important, the results highlight specific effects of (S)-ketamine but not (R)-ketamine on increases in metabolic activity, dopamine tone, and opioid receptor signaling in the mPFC.

Selective effects of (S)-ketamine on locomotor activity, CPP, and self-administration

Exposure to subanesthetic doses of ketamine in mice leads to increases in locomotor activity [61]. To test whether opioid receptors contribute to this behavioral effect, we pretreated male mice ($n = 8$ per group) with either saline or the opioid receptor antagonist naltrexone (10 mg/kg) followed by saline and then increasing doses of (S)-ketamine or (R)-ketamine (5, 10 and 20 mg/kg, IP, every 30 min) and measured their locomotor activity. We found that (S)-ketamine was more potent than (R)-ketamine in increasing locomotor activity, with R-ketamine increasing it only at the 20 mg/kg dose (Fig. 4A). More importantly, only the effects of (S)-ketamine were partially blocked by naltrexone. The mixed ANOVA, which included the between-subjects factor of naltrexone (0, 10 mg/kg) and the within-subjects factor of enantiomer dose (0, 5, 10, 20 mg/kg), showed significant effects of naltrexone

(F(5.791, 110.0) = 12.4, p<0.0001) and interaction between the two factors (F (69, 437) = 2.5, p<0.0001). These results suggest that subanesthetic doses of (S)-ketamine are sufficient to activate opioid receptors *in vivo*.

Next, we examined whether the two enantiomers differ in their effects on psychomotor sensitization, CPP, and intravenous drug self-administration, three classical behavioral procedures widely used to characterize the effects of opioid and psychostimulant drugs [62–63].

Psychomotor sensitization: First, we repeatedly injected male mice (n=12 per group) with vehicle (saline), (S)-ketamine, or (R)-ketamine, using a subanesthetic dose sufficient to induce locomotor activation for both enantiomers (20 mg/kg, IP), and measured locomotor activity for 3 days following two habituation days with saline injections (Figure 4B). As shown above, a 20 mg/kg IP injection of (S)- or (R)-ketamine increased locomotor activity; however, only mice injected with (S)-ketamine showed locomotor sensitization over days (Figure 4C-D). The mixed ANOVA, which included the between-subjects factor of drug condition (saline, (S)-ketamine, (R)-ketamine) and the within-subjects factor of day (days 1–3), showed significant effects of day (F(4, 84) = 31.2, p<0.0001), drug condition (F (2, 21) = 43.2, p<0.0001), and an interaction between the two factors (F (8, 84) = 16.6, p < 0.0001). Three days later, we injected all mice with escalating doses of (S)-ketamine (5, 10, 20 mg/kg, IP, every 30 min) in a single test session and assessed locomotor activity. Mice previously exposed to repeated (R)-ketamine injections did not differ from vehicle-treated mice, whereas mice that received repeated (S)-ketamine injections showed significantly higher locomotor activity compared to both (R)-ketamine- and vehicle-treated mice, indicating that they developed locomotor sensitization to (S)-ketamine. Furthermore, mice exposed to repeated (R)-ketamine injections did not cross-sensitize to (S)-ketamine (Figure 4D). The mixed ANOVA, which included the between-subjects factor of previous drug treatment (saline, (S)-ketamine, (R)-ketamine) and the within-subjects factor of time bin (5, 10, 15, 20, 25, 30 min) on test day, showed a significant drug treatment by time interaction (F (46, 483) = 1.9, p = 0.0007).

Conditioned place preference: Next, we tested the rewarding effects of (S)- and (R)-ketamine using the CPP procedure [62]. We injected male mice (n=9 per group) with either (S)- or (R)-ketamine (10 m/kg, IP) and placed them in one of two sides of a two-compartment chamber for 15 min. On alternate days, we injected the same mice with vehicle injections and placed them in the other side for 15 min (Figure 4B). We performed the drug or vehicle pairing over 6 days and counterbalanced the vehicle and drug injections during these days. The mice showed a significant preference for the (S)-ketamine-paired chamber but not for the (R)-ketamine-paired chamber (Figures 4E and 4F). The statistical analysis of the CPP score (the time spent in the drug-paired compartment), which included the between-subjects factor of enantiomer (R, S) and the within-subjects factor of session (pre-test, post-test), showed a significant effect of enantiomer (F (1, 16) = 4.7, p = 0.046) but not of session ((F (1, 16) = 3.0, p = 0.10) or interaction (F (1, 16) = 1.29, p = 0.27).

Self-administration: A previous study showed that rats self-administer racemic ketamine [27] but it is unknown if (S)- and (R)-ketamine are individually self-administered. We first

trained male and female rats (n = 15 to 20 per group; 6 to 8 females; 12 to 14 males) to self-administer (S)- or (R)-ketamine (0.5 mg/kg/infusion, dose based on ref. [27], for 16 days under a fixed-ratio 1 (FR1) reinforcement schedule with a 20-s timeout (Figure 4G). There were no statistically significant sex differences on any of the measures. Thus, we combined data from males and females and sex was not used as a factor in the statistical analyses.

We found that both male and female rats self-administered (S)-ketamine with a significant escalation of drug intake during the 16 training sessions (1-h per day) (Figure 4H). In contrast, the self-administration of (R)-ketamine was weaker and less reliable (Figure 4H-J). The statistical analysis of number of infusions per day, which included the between-subjects factor of enantiomer (R, S) and the within-subjects factor of session (1–16), showed significant main effects of enantiomer ($F(1, 555) = 64.8$, $p < 0.0001$), session ($F(15, 555) = 23.1$, $p < 0.0001$), and interaction ($F(15, 555) = 8.7$, $p < 0.0001$). Once the rats' self-administration behavior was stable (defined as less than 20% variation between three consecutive sessions), we analyzed the preference for the active versus inactive lever to evaluate possible non-specific responding (Figure 4J). The statistical analysis of number of responses, which included the between-subjects factor of enantiomer (R, S) and the within-subjects factor of lever (1–16), showed significant effects of enantiomer ($F(1, 60) = 50.6$ $p < 0.0001$), lever ($F(1, 60) = 102.5$, $p < 0.0001$), and interaction ($F(1, 60) = 38.7$, $p < 0.0001$).

The rats trained to self-administer (S)-ketamine also showed the characteristic inverted U-shaped dose response curve (maintaining their average intake at ~15 mg/kg/h), similar to other reinforcing substances with known abuse liability like heroin or cocaine [63]. In contrast, the rats trained to self-administer (R)-ketamine did not show this pattern of responding (Figure 4K). The analysis of number of infusions, which included the between-subjects factor of enantiomer and the within-subjects factor of dose (0.125, 0.25, 0.5, 1.0 mg/kg/infusion), showed significant effects of enantiomer ($F(1, 21) = 10.9$, $p = 0.0034$), dose ($F(3, 63) = 4.5$, $p = 0.0065$), and interaction ($F(3, 63) = 8.203$, $p = 0.0001$).

To further assess the reinforcing effects of (S)-ketamine and (R)-ketamine, we tested the rats on a progressive ratio schedule, a measure of the reinforcing effects of drugs in which each successive drug infusion requires an increasing number of active lever presses [64]. The rats trained to self-administer (S)-ketamine showed a significantly higher number of drug infusions than rats trained to self-administered (R)-ketamine (Figure 4L). The statistical analysis of the number of infusions, which included a between-subjects factor of enantiomer, showed a significant main effect of enantiomer ($t(22)=5.9$, $p < 0.0001$).

After the progressive ratio testing, we retrained the rats on the FR1 20-s timeout reinforcement schedule. Once they showed stable self-administration, we tested them for extinction of drug self-administration, a measure of drug seeking in studies using rat models of relapse [65]. There were no differences in extinction responding between the rats previously trained to press for (S-) and (R)-ketamine and both groups showed rapid extinction of drug seeking (Figure 4M). The analysis, which included the between-subjects

factor of enantiomer and the within-subject factors of extinction session, did not show significant effects of enantiomer, session, or interaction (p values > 0.05).

In sum, our results show that in mice low, subanesthetic doses of (S)-ketamine but not (R)-ketamine acutely induced locomotor activity that was decreased by pretreatment with the opioid antagonist naltrexone. Similarly, repeated injections of (S)-ketamine but not (R)-ketamine induced psychomotor sensitization and CPP in male mice. Additionally, male and female rats showed reliable escalation of intravenous (S)-ketamine self-administration, higher progressive ratio responding, and the characteristic inverted U-shaped dose-response curve. In contrast, male and female rats did not reliably self-administer (R)-ketamine and did not show the characteristic changes in drug self-administration as a function of changes in the drug's unit dose. Finally, neither enantiomer showed the characteristic time-dependent decreases in extinction responding that are typically observed with opioid and psychostimulant drugs.

Discussion

We studied the pharmacological and behavioral effects of (S)-ketamine and (R)-ketamine in mice and rats. We report four main findings. First, results from receptor binding assays indicate that both enantiomers bind to NMDARs, with (S)-ketamine showing higher affinity that (R)-ketamine. Additionally, both enantiomers bound to and activated MORs and KORs, with (S)-ketamine showing higher affinity and potency than (R)-ketamine. In contrast, (R)-ketamine bound to sigma-1 and sigma-2 receptors with higher affinity than (S)-ketamine. Second, results from PET and *ex vivo* uptake experiments and target deconvolution results indicate that (S)- and (R)-ketamine lack high affinity binding targets and exhibit negligible off-target binding profiles. Third, results from FDG and [^{18}F]fallypride PET experiments show that low, subanesthetic IV doses of (S)- or (R)-ketamine caused divergent regional changes in both brain metabolic activity and dopamine tone. Additionally, [^{35}S]GTPγS autoradiography showed that a physiologically-relevant concentration of (S)- or (R)-ketamine led to divergent activation of opioid receptors in the mPFC. These results highlight specific effects of (S)-ketamine but not (R)-ketamine on increases in metabolic activity, dopamine tone, and opioid receptor signaling in the mPFC. Finally, (S)-ketamine but not (R)-ketamine induced psychomotor sensitization and CPP in male mice and was intravenously self-administered by male and female rats. We discuss these results below.

Divergent pharmacological effects of (S)-ketamine and (R)-ketamine

Our biodistribution results are consistent with prior reports supporting stereoselective metabolic pathways of each enantiomer [42], where (R)-ketamine showed a slower rate of metabolism and longer half-life than (S)-ketamine. This finding could explain the higher [^{3}H](R)-ketamine brain uptake that we observed in our study. Our screening and target deconvolution findings preclude the existence of previously unidentified high-affinity targets for (S)- or (R)-ketamine. However, our radioligand binding and signaling results indicate not only quantitative differences in potency, but also a qualitatively divergent and complex target engagement profile between ketamine's two enantiomers, which involve NMDARs, as well as MORs, KORs, and sigma receptors. Specifically, we found that (S)-ketamine showed

higher affinity and potency for opioid receptors but lower affinity for sigma receptors compared to (R)-ketamine.

Ketamine's inhibition at the NMDAR has been traditionally attributed to its antidepressant effects [2, 19–22]. However, recent studies have implicated opioid receptors in the antidepressant-like behavioral and cellular effects of ketamine in rats [47] and in the antidepressant effects of ketamine in humans [49–50]. However, another human study failed to show a similar association [78], though this finding has been challenged [79]. The complex pharmacological profile of ketamine and its enantiomers would be expected to preclude the selective involvement of opioid receptors, NMDARs, or sigma receptors in these antidepressant-like (rodents) or antidepressant (human) effects. This is because low ketamine doses induce antidepressant effects and ketamine enantiomers show divergent modes of action at each target (i.e., inhibition at NMDAR but activation at opioid receptors, so at low doses it would be expected that opioid receptor activation would be equivalent or may even override NMDAR inhibition). Indeed, given that ketamine is an antagonist at NMDARs, the occupancy levels of ketamine required to antagonize ligand-induced NMDAR activation would be expected to be higher than the occupancy levels required to initiate a MOR or KOR signaling cascade. Furthermore, ketamine efficacy has also been associated with endogenous opioid activity [80]. Therefore, opioid receptor-dependent effects of (S)-ketamine may not be limited to the direct effects of the drug on opioid receptors but may also be due to a combination of MOR/KOR agonism/partial agonism and endogenous opioid release. In any case, our results support the notion that the selectivity exhibited by either enantiomer at any one of these targets is small and likely of limited *in vivo* relevance.

The mPFC has been implicated in both depression and substance use disorders [54, 55]. Our experiments revealed a consistent and selective bias for (S)-ketamine over (R)-ketamine to activate the mPFC, increase mPFC dopamine tone, and to increase mPFC MOR activity. Notably, these effects were observed at doses and concentrations previously shown to be sufficient for achieving antidepressant-like efficacy in rodent models [18, 71–73]. These findings are also consistent with prior PET imaging studies in humans, where (S)-ketamine (but not equivalent doses of (R)-ketamine) increased frontal cortex activity [81, 82]. Our results are also consistent with a pharmacological fMRI study in awake rats where a 10 mg/kg IP dose of (S)-ketamine but not (R)-ketamine increased cerebrovascular responses in the frontal cortex and other brain regions [83]. Therefore, (S)-ketamine action in the mPFC may not only be relevant for its antidepressant-like efficacy but also for its abuse liability profile.

The dissociation between the regional effects on brain activity and dopamine tone between the two enantiomers is intriguing and may be relevant to the selective (S)-ketamine effects on locomotor sensitization, CPP, and self-administration, as well as the reported greater antidepressant-like efficacy of (R)-ketamine over (S)-ketamine in rodent models of depression [17]. Unlike (S)-ketamine, (R)-ketamine was associated with inhibition of medial thalamic areas (including habenula). Similar regional decreases in cerebrovascular responses after (R)-ketamine have been previously observed [83]. Hyperexcitability of the habenula has been implicated in the development of MDD [72] and intrahabenular injections of ketamine in rodents reduce habenula activity and depression-like behaviors [72]. However,

double-blind placebo-controlled clinical trials are necessary to confirm the antidepressant efficacy of (R)-ketamine in humans [18, 73].

Divergent behavioral effects of (S)-ketamine and (R)-ketamine

Based on (S)-ketamine's pharmacological profile, we reasoned that the drug would exhibit higher potential liability for abuse than (R)-ketamine [56–58, 66]. To test this hypothesis, we performed a series of behavioral studies. Our results showed that (S)-ketamine but not (R)-ketamine induced locomotor activity that was opioid receptor-dependent. Furthermore, like opioid and psychostimulant drugs [65, 67], mice developed psychomotor sensitization to repeated injections of (S)-ketamine but not (R)-ketamine. These findings are consistent with a recent study showing that repeated intermittent injections (10 mg/kg/day, twice weekly for 8 weeks) of (S)-ketamine but not (R)-ketamine led to increased methamphetamine-induced locomotion in mice [68]. In agreement with a prior study [69], we also found that an antidepressant-like dose of (S)-ketamine but not (R)-ketamine induced CPP in mice [69].

Our observations from the drug self-administration procedures in rats (where we implemented multiple behavioral measures and doses), suggest that (S)-ketamine has significantly greater potential for abuse liability than (R)-ketamine. Specifically, we found that (S)-ketamine was a reliable operant reinforcer in the drug self-administration procedure. In particular, unlike rats that self-administered (R)-ketamine, rats that self-administered (S)-ketamine significantly increased (escalated) their drug intake over days, showed the characteristic inverted U-shaped dose-response curve, and increased the response requirements under the progressive ratio schedule. Despite this, rats that self-administered either enantiomer (especially (S)-ketamine) showed rapid extinction of self-administration. The reasons for the rapid decrease in extinction responding to both enantiomers are unknown but this observation indicates that (S)- and (R)-ketamine would not be expected to induce similar conditioned responses as opioid or psychostimulant drugs, which are known to promote drug relapse in humans and rat models after prolonged abstinence [65,70]. One speculative translational implication of our rapid extinction data is that recreational non-medical use (S)-ketamine is less likely to result in a substance use disorder (as defined by DSM-5) than opioid or psychostimulant drugs.

Overall, the findings from the drug self-administration procedure are particularly important because results from this procedure predict abuse liability of drugs in humans, because many drugs whose recreational use can lead to substance use disorder in some humans are self-administered by laboratory rodents and monkeys [32, 36].

Methodological considerations

Our study has some limitations. We only used a single dose of each enantiomer in the CPP procedure and a prior study [71] showed that a higher (40 mg/kg IP) dose of (R)-ketamine produced CPP in mice. However, this same dose of (R)-ketamine did not produce CPP in a different study (68) and this dose was 4 times the dose needed (typically 10 mg/kg) to elicit antidepressant-like effects in mice and rats [19, 72–73].

Humans and rodents differ across many physical, metabolic, and physiological domains. Therefore, it is difficult to make direct comparisons between doses that are efficacious

in each species. One approach that is typically used to make comparative dose estimates involves the use of body surface area [74]. According to this method, a 10 mg/kg dose in a mouse (considered an antidepressant-like dose [19]) is estimated at a human equivalent dose of ~0.8 mg/kg, which approximates the 0.5 mg/kg dose of ketamine used in humans [74].

Regarding our measures of dopamine tone, a prior PET study in awake monkeys reported decreases in [^{11}C]raclopride binding (i.e. increased dopamine tone) after intravenous injection of (S)-ketamine but not to (R)-ketamine [59]. Here we did not see any effects of either (S)-ketamine or (R)-ketamine on striatal dopamine tone using [^{18}F]fallypride (a different D2/D3 PET radioligand). This discrepancy may be due to the different doses, species, and perhaps differences in displacement sensitivity between the two PET ligands [75].

Clinical implications

Our results showing reliable self-administration of (S)-ketamine in rats of both sexes, may be relevant to concerns previously raised for the clinical use of (S)-ketamine (Spravato® nasal spray is self-administered by patients during treatment [76]), especially in patients with comorbid substance use disorders [33]. Furthermore, our findings may also have potential clinical implications for the use of (R)-ketamine in the treatment of depression. Specifically, if current clinical trials indicate that (R)-ketamine shows antidepressant efficacy, our results will predict that this enantiomer may have a more favorable risk/benefit treatment profile than (S)-ketamine, especially in patients with comorbid substance use disorders. This notion is tentatively supported by a recent study in mice which showed that (R)-ketamine decreases morphine CPP and naloxone-precipitated opioid withdrawal [77].

Methods

Binding and enzyme target profile screen

These experiments were performed by an outside vendor (Eurofins, France). Briefly, membrane homogenates from stable cell lines or rat tissues expressing each receptor/enzyme were incubated with the respective radioligand in the absence or presence of (S-) and (R)-ketamine (100 nM and 10 μM). In each experiment, the respective reference compound was tested concurrently with the test compound to assess the assay reliability. Nonspecific binding was determined in the presence of a specific agonist or antagonist at the target. Following incubation, the samples were filtered rapidly under vacuum through glass fiber filters presoaked in buffer and rinsed several times with an ice-cold buffer using a 48-sample or 96-sample cell harvester. The filters were counted for radioactivity in a scintillation counter using a scintillation cocktail.

Radioligand binding experiments

Dissected rat brains (except the cerebellum) was cut and suspended in Tris-HCl 50 mM buffer supplemented with protease inhibitor cocktail (1:1000) and disrupted with a Polytron homogenizer (Kinematica, Basel, Switzerland). Homogenates were centrifuged at 48,000g (50 min, 4 °C) and washed twice in the same conditions to isolate the membrane fraction. Protein was quantified by the bicinchoninic acid method (Pierce). For competition

experiments, membrane suspensions (50 or 100 μg of protein/ml) were incubated with a constant amount of radioligand and the indicated increasing concentrations of the competing drugs during 2 h at RT. Nonspecific binding was determined in the presence of an exceeding concentration of cold ligand. In all cases, free and membrane-bound radioligand were separated by rapid filtration of 500-μl aliquots in a 96-well plate harvester (PerkinElmer, Boston, MA, USA) and washed with 2 ml of ice-cold Tris-HCl buffer. Microscint-20 scintillation liquid (65 μl/well, PerkinElmer) was added to the filter plates, plates were incubated overnight at RT and radioactivity counts were determined in a MicroBeta2 plate counter (USA) with an efficiency of 41%. One-site competition curves were fitted using Prism 7 (GraphPad Software, La Jolla, CA, USA). Ki values were calculated using the Cheng–Prusoff equation.

For NMDAR binding, membrane preparations were incubated with 5 mM Tris-HCl (pH 7.4) containing glutamate (100 μM), glycine (100 μM), [^{3}H](+)-MK-801 (5 nM, 30 Ci/mmol, Novandi) and increasing concentrations (0.1 nM to 1 mM) of competing compounds: (S)-ketamine and (R)-ketamine. Non-specific binding was determined in the presence of 1 mM of unlabeled (+)-MK-801. For Sigma-1 binding, membrane preparations were incubated with 50 mM Tris-HCl (pH 8) containing [^{3}H](+)pentazocine (3 nM, 28.34 Ci/mmol, Perkin Elmer) and increasing concentrations (10 nM to 10 mM) of competing compounds. Non-specific binding was determined in the presence of 100 μM of unlabeled haloperidol. For Sigma-2 binding, membrane preparations were incubated with 50 mM Tris-HCl (pH 7.4) containing [^{3}H]-(1,3-di-*o*-tolylguanidine) (DTG) (2 nM, 40 Ci/mmol, Perkin Elmer), pentazocine (100 nM, to block Sigma-1 binding), and increasing concentrations (10 nM to 10 mM) of competing compounds. Non-specific binding was determined in the presence of 100 μM of unlabeled DTG. For MOR binding, membrane preparations were incubated with 50 mM Tris-HCl (pH 7.4) containing [^{3}H]DAMGO (1 nM, NIDA Drug Supply) and increasing concentrations (10 nM to 1 mM) of competing compounds. Non-specific binding was determined in the presence of 100 μM of unlabeled DAMGO. For KOR binding, membrane preparations were incubated with 50 mM Tris-HCl (pH 7.4) containing [^{3}H]U69,593 (1 nM, 36 Ci/mmol, Novandi) and increasing concentrations (10 nM to 1 mM) of competing compounds. Non-specific binding was determined in the presence of 100 μM of unlabeled U69,593.

In vitro signaling experiments

Human embryonic kidney (HEK-293, ATCC) cells were grown in Dulbecco's modified Eagle's medium (DMEM; Gibco, ThermoFisher Scientific, Waltham, MA, USA) supplemented with antibiotic/antimycotic (all supplements from Gibco) and 10% heat-inactivated fetal bovine serum (Atlanta Biologicals, Inc. Flowery Branch, GA, USA) and kept in an incubator at 37 °C and 5% CO2. Cells were routinely tested for myclopasma contamination (MycoAlert® Mycoplasma Detection Kit, Lonza). Cells were seeded on 60 cm^2 dishes at 4 × 10^6 cells/dish 24 h before transfection. The indicated amount of cDNA was transfected into HEK-293 cells using polyethylenimine (PEI; Sigma-Aldrich) in a 1:3 DNA:PEI ratio. Cell harvesting for radioligand binding experiments or signaling assays were performed approximately 48 h after transfection.

Two different types of BRET assays were used to determine signaling at the receptor: cAMP accumulation and β-arrestin recruitment. cAMP accumulation was measured by employing the CAMYEL biosensor (cAMP sensor using YFP-Epac-Rluc). Cells were transfected with 5 μg of untagged receptor (MOR or KOR) and 5 μg of CAMYEL biosensor using the PEI method described above. For β-arrestin recruitment BRET, cells were transfected with 1 μg of MOR-Rluc8 or KOR-Rluc8, 5 μg of β-arrestin2-mVenus and 5 μg of GRK2. On experiment day, cells were harvested, washed and resuspended in DPBS containing 5.5 mM glucose. Cells were then plated in 96-well white solid bottom plates (Greiner bio-One) and incubated in the dark for 45 min. Dose-response curves were performed by adding coelenterazine h (5 μM, Nanolight Technology) for 5 minutes followed by addition of the indicated concentrations of compounds for 10 (cAMP) or 20 (β-arrestin) minutes. For cAMP accumulation experiments, 10 μM Forskolin was added to the cells and incubated for 5 minutes before coelenterazine addition. BRET signal was determined by calculating the ratio of the light emitted by mVenus (535/30 nm) over that emitted by Rluc8 (475/30 nm) using a Pherastar plate reader (BMG Labtech, Cary, NC). Net BRET values were obtained by subtracting the BRET ratio from cells treated with vehicle. Agonist-promoted BRET changes were expressed as % morphine maximum response. Fluorescence levels were also monitored to control for expression across experiments by plating cells in 96-well black solid bottom plates (Greiner Bio-One) and measuring mVenus emission (480/530).

Ex vivo GTPγS

Flash frozen tissue was sectioned (10 μm) on a cryostat (Leica) and thaw mounted on ethanol cleaned glass slides. Sections were encircled with a hydrophobic membrane using a PAP pen (Sigma-Aldrich). Preincubation buffer (50 mM Tris-HCl, 1 mM EDTA, 5 mM MgCl2, and 100 mM NaCl) was pipetted onto each slide and allowed to incubate for 20 min). The preincubation buffer was removed via aspiration and each slide was loaded with GDP in the presence of DPCPX and allowed to incubate of 60 min (Preincubation buffer, 2 mM GDP, 1 μM DPCPX, Millipore water). GDP buffer was removed via aspiration and [^{35}S]GTPγS cocktail (GDP buffer, 1.3 mM DTT, 2.7 mM GDP, 1.3 μM DPCPX, 83 pM [^{35}S]GTPγS) with the indicated drugs (morphine 1 μM or the ketamine enantiomers 10 μM), without drugs (basal condition), or with a saturated concentration of nonradioactive GTP (for nonspecific binding) was pipetted onto each slide and allowed to incubate for 90 min. In case of antagonist pre-treatment, the slides were incubated with pre-incubation buffer containing naloxone (10 μM) for 10 minutes before the addition of the [^{35}S]GTPγS cocktail containing the indicated drug plus naloxone (10 μM). The [^{35}S]GTPγS cocktail was removed via aspiration and slides were washed in ice-cold washing buffer (50 mM Tris-HCl, 5 mM $MgCl_2$, pH 7.4) for 5 min (2×) followed by a 30 s dip in ice-cold deionized water. Hydrophobic membrane was removed with a cotton swab and xylene and slides were placed into a Hypercassette™ covered by a BAS-SR2040 phosphor screen (FujiFilm; GE Healthcare). The slides were exposed to the phosphor screen for 3–5 days and imaged using a phosphor imager (Typhoon FLA 7000; GE Healthcare).

[^{11}C]-ketamine PET

Rats were anesthetized with isoflurane and placed in a prone position on the scanner bed of an ARGUS small animal PET/CT (Sedecal, Spain) and injected intravenously (in 70 to 150

μl of saline) with [^{11}C](S)-ketamine (30–50 MBq, 450–520 kBq/μmol, Johns Hopkins PET Center) or [^{11}C](R)-ketamine (30–50 MBq, 450–520 kBq/μmol, Johns Hopkins PET Center) and dynamic scanning commenced. When indicated, animals were pretreated (5 min before the injection of the PET radiotracer) with vehicle or MK-801 (1 mg/kg, IP), (S)-ketamine (10 mg/kg, IP) or (R)-ketamine (10 mg/kg, IP. Total acquisition time was 60 min.

The PET data were reconstructed and corrected for dead-time and radioactive decay. All qualitative and quantitative assessments of PET images were performed using the PMOD software environment (PMOD Technologies, Zurich Switzerland). The dynamic PET images were coregistered to MRI templates and time-activity curves were generated using PMOD's built-in atlases and the described analyses were performed. Standardized uptake value (SUV) was calculated as using the equation SUV = C / (dose / BW) where C is the tissue concentration of [^{11}C]ketamine (kBq/cc), *dose* is the administered dose (MBq) and *BW (kg)* is the animal's body weight. Statistical analyses were performed using Prism 7 (GraphPad Software, La Jolla, CA, USA).

Ex vivo biodistribution

Male and female rats (2 per condition) were injected (IV, 1μCi/g) with radiolabeled [^{3}H]-(S)-ketamine or [^{3}H]-(R)-ketamine and euthanized at 10, 30, 40, or 60 min post injection and brain, blood, and tissues were collected for radiometric analyses. The brains were flash frozen in 2-methylbutane and stored at −80ºC until use. The blood was centrifuged (13,000 rpm, 10 min at RT) and serum was collected. The tissues were bleached with hydrogen peroxide and solubilized (Solvable, Perkin Elmer). Serum and tissue samples (were dissolved in scintillation cocktail (2.5 mL) and radioactivity counts were determined using a liquid scintillation counter.

The brains were sectioned (20 μm) on a cryostat (Leica), mounted into glass microscope slides and air-dried overnight at RT. The day after slides were placed into a Hypercassette™ covered by a BAS-TR2025 phosphor screen (FujiFilm; GE Healthcare). The slides were exposed to the phosphor screen for 10–15 days and imaged using a phosphor imager (Typhoon FLA 7000; GE Healthcare). The digitized images were calibrated using C-14 standard slides (American Radiolabeled Chemicals). ROIs were hand-drawn based on anatomical landmarks and radioactivity was quantified using ImageJ. The activity in 6 to 10 different sections was averaged per each animal and brain region.

[^{18}F]-Fluorodeoxyglucose PET

This procedure was based on previous studies [84, 85]. Rats were habituated to experimenter handling and the open field arena. Rats were fasted 16 h before the experiment. On the day of the experiment, rats received a continuous IV infusion of vehicle (buffered saline), (S)-ketamine (10 mg/kg), or (R)-ketamine (10 mg/kg) over 40 min in an open field arena. Ten minutes after start of infusion, rats were injected (IP) with 13 MBq of 2-deoxy-2-[^{18}F]fluoro-D-glucose (FDG; Cardinal Health). After 30 min, rats were anesthetized with 1.5% isoflurane, placed on a custom-made bed of a nanoScan small animal PET/CT scanner (Mediso Medical Imaging Systems) and scanned for 20 min on a static acquisition protocol, followed by a CT scan. The PET data were reconstructed and

coregistered to an MRI template as described above. All statistical parametric mapping analyses were performed using Matlab R2016 (Mathworks) and SPM12 (University College London).

[^{18}F]-Fallypride PET

Rats were habituated to experimenter handling and the open field arena. On the day of the experiment, rats were injected (IV) with 13 MBq of [^{18}F]Fallypride (Johns Hopkins University) right before receiving a continuous IV infusion of vehicle (buffered saline), (S)-ketamine (10 mg/kg), or (R)-ketamine (10 mg/kg) for 40 min in an open field arena. Rats were anesthetized with 1.5% isoflurane, placed on a custom-made bed of a nanoScan small animal PET/CT scanner (Mediso Medical Imaging Systems) and scanned for 30 min on a static acquisition protocol, followed by a CT scan. The PET data were reconstructed and coregistered to an MRI template as described above. Coregistered images were analyzed using one-way ANOVA and the resulting parametric images were filtered for statistically significant ($p < 0.05$) clusters larger than 100 contiguous voxels. All statistical parametric mapping analyses were performed using Matlab R2016 (Mathworks) and SPM12 (University College London).

General animal handling

Male wild-type mice (C57BL/6J) were ordered from the Jackson Laboratory, weighing 20 to 25 g. Mice were maintained under a normal 12-hour light/dark cycle with food and water freely available. Male and female Sprague-Dawley rats (strain code #400) were ordered from Charles River Laboratories, weighing 200 to 250 g. Rats were maintained under a reverse 12-hour light/dark cycle with ad libitum access to food and water. We housed two rats per cage before surgery and individually after surgery. Rats feeding regimen was restricted to 18 to 20 g per day throughout the experiment task in order to maintain a stable weight of the rats and facilitate acquisition of drug self-administration. All experiments and procedures complied with all relevant ethical regulations for animal testing and research and followed the National Institutes of Health (NIH) guidelines and were approved by each institute's animal care and use committees. The experimenters were blind to the group allocation during data acquisition.

Locomotor activity in mice

Male wild-type mice (C57BL/6J, 20–25 g, N=32) were tested for ketamine-induced locomotor activity. The mice were injected with saline followed by increasing doses of (S)- or (R)-ketamine (5, 10 and 20 mg/kg. IP). A subset of mice (N=16, 8 per group) was injected with naltrexone-HCl (10 mg/kg, IP) 10 min before saline or (S)- or (R)-ketamine injections. After the injections, the mice were placed immediately in an open field arena (Opto-varimex ATM3, Columbus Instruments). Locomotor activity was tracked for 120 min as infrared beam crossing and traveled distance were converted to m and binned into 5 min time-bins.

Cross-sensitization in mice

Male wild-type mice (C57BL/6J, 20–25 g, N=24) were tested for ketamine-induced locomotor sensitization. The locomotor sensitization experiment was divided into three phases: habituation, induction, and expression. During habituation, mice were injected with saline (0.9% NaCl) for two consecutive days. For the induction phase, mice were injected with saline (n=8), (S)-ketamine (20 mg/kg, n=8), or (R)-ketamine (20 mg/kg, n=8) for three consecutive days. Three days later, all mice were injected with saline followed by increasing doses of (S)-ketamine (5, 10, and 20 mg/kg). All drugs were administered IP and mice were placed immediately in an open field arena (Opto-varimex ATM3, Columbus Instruments) after injection. Locomotor activity was tracked for 30 min (on habituation and induction phases) or 120 min (on expression day) as infrared beam crossing and traveled distance were converted to m.

Conditioned place preference in mice

The task consisted of 8 sessions, 1 per day, in chambers with two visually distinct sides, one with clear walls and white floor and one with checkered walls and black floor. The sides were separated by a wall with a center pass. Locomotor activity was measured by way of time spent in each chamber as well as total distance traveled (Opto-varimex ATM3, Columbus Instruments). In the first session, the mice could freely explore both sides of a conditioning box for 20 min to determine inherent side preference, designated as the Pre-Test. Using this data, the drug-paired side was pseudo-randomized so, on average, they did not show preference for either side. Mice with no side preference were ketamine-paired in a counterbalanced fashion. In an alternating fashion for 6-days, mice were injected (IP) with either saline (n=8), (S)-ketamine (10 mg/kg, n=8), or (R)-ketamine (10 mg/kg, n=8) and placed in the predetermined drug/no drug side of the chamber for 20 min. In the last session (designated as Post-Test) the animals had access to both sides during 10 min, and their CPP score was quantified as: $(T_D - T_V) / T$, where T_D and T_V are the times spent in the drug paired chamber and the vehicle paired chamber, respectively, and T is the total duration of the session.

Self-administration in rats

Intravenous surgery—The procedure is based on previous studies [86]. Rats were anesthetized with isoflurane (5% induction; 2–3% maintenance). Catheters were made from Silastic tubing attached to a modified 22-gauge cannula (Plastics One, Cat# C313G-5up) and cemented to polypropylene mesh (Elko Filtering Co., Cat# 05–1000/45). The catheter was inserted into the jugular vein, and the mesh was fixed to the mid-scapular region of the rat. Rats were injected with carprofen (2.5 mg/kg, SC, Norbrook) after surgery and on the following day to relieve pain and decrease inflammation. Rats recovered for 6–8 days before drug self-administration training. During all experimental phases, catheters were flushed daily with gentamicin (4.25 mg/mL, Fresenius Kabi, Cat# 1002) dissolved in sterile saline. If we suspected catheter failure, we tested patency with a short-acting barbiturate anesthetic Brevital (methohexital sodium, 10 mg/mL in buffered saline, 0.1–0.2 mL injection volume, IV).

Apparatus—All rats were trained and tested in standard Med Associates self-administration chambers. Each chamber had either one or two levers located 7.5–8 cm above the grid floor. Lever presses on the active, retractable lever activated the infusion pump, whereas lever presses on the inactive, retractable lever had no consequences. Each session began with the illumination of a house light that remained on for the entire session. The active and inactive lever was inserted into the chamber 10 s after the house light was illuminated. During the self-administration sessions, a fixed-ratio-1 (FR1) reinforcement schedule (each lever press is reinforced) was used. Each infusion was paired with a 20-s white-light cue and there was a 20-s timeout before responses resulted in another infusion. At the end of the session, the house light was turned off and levers were retracted.

Ketamine self-administration training—Several cohorts of male and female rats were trained to self-administer (S)-ketamine (Toronto Research Chemicals, Cat# K165310) or (R)-ketamine (Toronto Research Chemicals, Cat# K165305) during 3 h/day (three 1 h sessions separated by 10 min) or 1 h/day for 16 days. In all cases, ketamine was infused over 3.5 s at a dose of 0.5 mg/kg/infusion. Responses on the active lever during the timeout period were recorded but did not result in ketamine infusions. Responses on the inactive lever were recorded but had no consequences. Two cohorts of rats were trained for food self-administration. [Note: Prior food self-administration allows to dissociate between the subsequent drug's reinforcing effects in the operant self-administration procedures and the drug's effects on operant learning, which are confounded in rats without prior operant training.] These rats were responding for food on the lever that later became the 'inactive' lever for ketamine self-administration. Hence, a subset of rats did not have the inactive lever available during training phase (and no difference was observed in their responses to the active lever or infusions of ketamine obtained per session). In this subset of rats, the inactive lever was re-introduced in the testing phases described below. In all cases, rats were considered trained if there was less than 20% variation in their infusions per session during consecutive daily sessions. The data from rats that did not meet this criterion or that did not pass the catheter patency test were excluded from the study (3 rats were excluded from the (S)-ketamine group and 4 rats were excluded from the (R)-ketamine group). After last training session, the rats were divided into two separate testing groups to perform the experiments described below.

Dose response—One cohort (n=8/condition) was placed on a multiple-dose schedule to observe dose-dependent ketamine self-administration according to a randomized ketamine dose sequence (0.125, 0.25, 0.5, or 1.0 mg/kg/infusion) for 1 h/day for 8 days. All parameters (reinforcement schedule, light cues, etc.) remained the same as training, except for drug dose. The number of ketamine infusions earned, active, and inactive lever responses were recorded for each session.

Progressive Ratio—Another cohort (n=8/condition) were trained for 3 days on a progressive ratio (PR) reinforcement schedule (6 h/day, 0.5mg/kg/infusion). The number of lever presses needed to receive a ketamine infusion was raised progressively within each session according to the following sequence: 2, 4, 6, 9, 12, 15, 20, 25, 32, 40, 50, 62, 77, 95, 118, 145, 178, 219, etc [45] until the break point was reached. The break point was defined

as the last schedule requirement completed for a ketamine infusion prior to a 30 min period during which no infusions were obtained.

Extinction—Following progressive ratio testing, the same rats were retrained to self-administer (S)- or (R)-ketamine (0.5 mg/kg/infusion) on an FR1 reinforcement schedule for 3 h/day for 3 days. During extinction, active lever presses resulted in saline infusions with all the cues present. Lever presses were recorded but did not result in ketamine infusions. The extinction phase continued for 3 h/day for 5 days.

Supplementary Material

Refer to Web version on PubMed Central for supplementary material.

Acknowledgements

This work was supported by NIDA (ZIA000069), NIMH and NINDS intramural funds. We thank Drs. Marisela Morales (NIDA/IRP), Martin Pomper (Johns Hopkins University) and Robert Dannals (Johns Hopkins University) for providing resources and equipment that made this work possible. We also thank the technical support provided by Theresa Kopajtic, Hannah Korah and Sarah Applebey in helping us set up experimental procedures.

CAZ is listed as a co-inventor on a patent for the use of ketamine in major depression and suicidal ideation. CAZ is listed as co-inventor on a patent for the use of (2R,6R)- hydroxynorketamine, (S)-dehydronorketamine, and other stereo- isomeric dehydro and hydroxylated metabolites of (R,S)-ketamine metabolites in the treatment of depression and neuropathic pain; and as a co-inventor on a patent application for the use of (2R,6R)-hydroxynorketamine and (2S,6S)-hydroxynorketamine in the treatment of depression, anxiety, anhedonia, suicidal ideation, and posttraumatic stress disorders. He has assigned his patent rights to the US government but will share a percentage of any royalties that may be received by the government.

References

1. Gao M, Rejaei D, Liu H, Ketamine use in current clinical practice. Acta Pharmacol Sin 37, 865–72 (2016). [PubMed: 27018176]
2. Berman RM, Cappiello A, Anand A, Oren DA, Heninger GR, Charney DS et al. , Antidepressant effects of ketamine in depressed patients. Biol Psychiatry 47, 351–354 (2000). [PubMed: 10686270]
3. Diazgranados N, Ibrahim L, Brutsche NE, Newberg A, Kronstein P, Khalife S et al. , A randomized add-on trial of an N-methyl-D-aspartate antagonist in treatment-resistant bipolar depression. Arch Gen Psychiatry 67, 793–802 (2010). [PubMed: 20679587]
4. Zarate CA, Singh JB, Carlson PJ, Brutsche NE, Ameli R, Luckenbaugh DA et al. , A randomized trial of an N-methyl-D-aspartate antagonist in treatment-resistant major depression. Arch Gen Psychiatry 63, 856–864 (2006). [PubMed: 16894061]
5. Zarate CA, Brutsche NE, Ibrahim L, Franco-Chaves J, Diazgranados N, Cravchik A.l et al. , Replication of ketamine's antidepressant efficacy in bipolar depression: a randomized controlled add-on trial. Biol Psychiatry 71, 939–946 (2012). [PubMed: 22297150]
6. Fava M, Freeman MP, M Flynn, Judge H, Hoeppner BB, Cusin C et al. , Double-blind, placebo-controlled, dose-ranging trial of intravenous ketamine as adjunctive therapy in treatment-resistant depression (TRD). Mol Psychiatry, (2018).
7. Singh JB, Fedgchin M, Daly EJ, Boer PD, Cooper K, Lim P et al. , A Double-Blind, Randomized, Placebo-Controlled, Dose-Frequency Study of Intravenous Ketamine in Patients With Treatment-Resistant Depression. Am J Psychiatry 173, 816–826 (2016). [PubMed: 27056608]
8. Murrough JW, Iosifescu DV, Chang LC, Al Jurdi RK, Green CE, M Perez A et al. , Antidepressant efficacy of ketamine in treatment-resistant major depression: a two-site randomized controlled trial. Am J Psychiatry 170, 1134–1142 (2013). [PubMed: 23982301]

9. aan het Rot M, Collins KA, W Murrough J, Perez AM, L Reich D, S Charney D et al. , Safety and efficacy of repeated-dose intravenous ketamine for treatment-resistant depression. Biol Psychiatry 67, 139–145 (2010). [PubMed: 19897179]
10. Carter LP and R Griffiths R, Principles of laboratory assessment of drug abuse liability and implications for clinical development. Drug Alcohol Depend. 105, 14–25 (2009)
11. Zhu W, Ding Z, Zhang Yinan, Shi Jie, Hashimoto Kenji, Lu Lin, Risks Associated with Misuse of Ketamine as a Rapid-Acting Antidepressant. Neurosci Bull 32, 557–564 (2016). [PubMed: 27878517]
12. Wang C, Zheng D, Xu J, Lam W, Yew DT, Brain damages in ketamine addicts as revealed by magnetic resonance imaging. Front Neuroanat 7, 23 (2013). [PubMed: 23882190]
13. US Food and Drug Administration, FDA approves new nasal spray medication for treatment-resistant depression; available only at a certified doctor's office or clinic. https://www.fda.gov/news-events/press-announcements/fda-approves-new-nasal-spray-medication-treatment-resistant-depression-available-only-certified (2019)
14. Janssen Announces U.S. FDA Approval of SPRAVATO® (esketamine) CIII Nasal Spray to Treat Depressive Symptoms in Adults with Major Depressive Disorder with Acute Suicidal Ideation or Behavior https://www.prnewswire.com/news-releases/janssen-announces-us-fda-approval-of-spravato-esketamine-ciii-nasal-spray-to-treat-depressive-symptoms-in-adults-with-major-depressive-disorder-with-acute-suicidal-ideation-or-behavior-301104437.html (2020)
15. Turner EH, Esketamine for treatment-resistant depression: seven concerns about efficacy and FDA approval. The Lancet 6, 977–979 (2019) [PubMed: 31680014]
16. Schatzberg AF, A Word to the Wise About Intranasal Ketamine. Am. J. Psychiatry 176, 422–424 (2019) [PubMed: 31109197]
17. Yang C, Shirayama Y, J-c Zhang, Ren Q, Yao W, Ma M et al. , (R)-ketamine: a rapid-onset and sustained antidepressant without psychotomimetic side effects. Transl Psychiatry 5, e632 (2015). [PubMed: 26327690]
18. Leal GC, Bandeira ID, Correia-Melo FS, Telles M, Mello RP, Vieira F, et al. , Intravenous arketamine for treatment-resistant depression: open-label pilot study. Eur Arch Psychiatry Clin Neurosci (2020)
19. Zanos P, Moaddel R, Morris PJ, Riggs LM, Highland JN, Georgiou P et al. , Ketamine and Ketamine Metabolite Pharmacology: Insights into Therapeutic Mechanisms. Pharmacol Rev 70, 621–660 (2018). [PubMed: 29945898]
20. Zorumski CF, Izumi Y, Mennerick S, Ketamine: NMDA Receptors and Beyond. J Neurosci 36, 11158–11164 (2016). [PubMed: 27807158]
21. Gupta A, Devi LA, Gomes I, Potentiation of μ-opioid receptor-mediated signaling by ketamine. J Neurochem. 119, 294–302 (2011) [PubMed: 21692801]
22. Nemeth CL, Paine TA, Rittiner JE, Béguin C, Carroll FI, Roth BL et al. , Role of kappa-opioid receptors in the effects of salvinorin A and ketamine on attention in rats. Psychopharmacology 210, 263–264 (2010) [PubMed: 20358363]
23. Itzhak Y, Simon EJ, A novel phencyclidine analog interacts selectively with mu opioid receptors. J Pharmacol Exp Ther 230, 383–386 (1984). [PubMed: 6086884]
24. He XS, Raymon LP, Mattson MV, Eldefrawi ME, de Costa BR, Synthesis and biological evaluation of 1-[1-(2-benzo[b]thienyl)cyclohexyl]piperidine homologues at dopamine-uptake and phencyclidine- and sigma-binding sites. J Med Chem 36, 1188–1193 (1993). [PubMed: 8098066]
25. Chaudieu I, Vignon J, Chicheportiche M, Kamenka JM, Trouiller G, Chicheportiche R, Role of the aromatic group in the inhibition of phencyclidine binding and dopamine uptake by PCP analogs. Pharmacol Biochem Behav 32, 699–705 (1989). [PubMed: 2544905]
26. Seeman P, Ko F, Tallerico T, Dopamine receptor contribution to the action of PCP, LSD and ketamine psychotomimetics. Mol Psychiatry 10, 877–883 (2005). [PubMed: 15852061]
27. De Luca M, Badiani A, Ketamine self-administration in the rat: evidence for a critical role of setting, Psychopharmacology 214, 549–556 (2011) [PubMed: 21069515]
28. Morgan CAJ, Curran H, Independent Scientific Committee on Drugs, Ketamine use: a review. Addiction 107, 27–28 (2012) [PubMed: 21777321]

29. M Hillhouse T, Porter JH, Negus SS, Dissociable effects of the noncompetitive NMDA receptor antagonists ketamine and MK-801 on intracranial self-stimulation in rats. Psychopharmacology 231, 2705–2716 (2014) [PubMed: 24522331]
30. Yang C, Hashimoto K, Rapid antidepressant effects and abuse liability of ketamine. Psychopharmacology 231, 2041–2042 (2014) [PubMed: 24668037]
31. M Hillhouse T, Porter JH, Negus SS, Reply to: Rapid antidepressant effects and abuse liability of ketamine. Psychopharmacology 231, 2743–2744 (2014)
32. Brady JV Animal models for assessing drugs of abuse. Neurosci Biobehav Rev 15, 35–43. (1991) [PubMed: 2052196]
33. Hunt GE, Malhi GS, Xiong Lai HM, Cleary M, Prevalence of comorbid substance use in major depressive disorder in community and clinical settings, 1990–2019: Systematic review and meta-analysis J Affect Disord 266, 288–304 (2020) [PubMed: 32056890]
34. Wise RA and Bozarth MA, A psychomotor stimulant theory of addiction. Psychol Rev 94, 469–92 (1987) [PubMed: 3317472]
35. Bardo MT and Bevins RA, Conditioned place preference: what does it add to our preclinical understanding of drug reward? Psychopharmacology 153, 31–43 (2000) [PubMed: 11255927]
36. R Schuster C and Thompson T, Self administration of and behavioral dependence on drugs. Annu Rev Pharmacol 9, 483–502 (1969) [PubMed: 4978013]
37. Shiue CY et al. , Carbon-11 labelled ketamine-synthesis, distribution in mice and PET studies in baboons Nucl Med Biol. 24, 145–50 (1997) [PubMed: 9089707]
38. Hartvig P, Valtysson J, Antoni G, Westerberg G, Långström B, Ratti Moberg E et al. , Brain kinetics of (R)- and (S)-[N-methyl-11C]ketamine in the rhesus monkey studied by positron emission tomography (PET) Nucl Med Biol. 21, 927–934 (1994) [PubMed: 9234346]
39. Kumlien E, Hartvig P, Valind S, Oye I, Tedroff J, Långström B, NMDA-receptor activity visualized with (S)-[N-methyl-11C]ketamine and positron emission tomography in patients with medial temporal lobe epilepsy. Epilepsia 40, 30–7 (1999) [PubMed: 9924899]
40. Murray F, Kennedy J, Hutson PH, Elliot J, Huscroft I, Mohnen K, et al. , Modulation of [3H]MK-801 binding to NMDA receptors in vivo and in vitro. European Journal of Pharmacology 397, 263–270 (2000) [PubMed: 10844123]
41. Herring BE, Xie Z, Marks J, Fox AP, Isoflurane Inhibits the Neurotransmitter Release Machinery J Neurophysiol. 102, 1265–1273 (2009) [PubMed: 19515956]
42. Portmann S, Kwan HY, Theurillat R, Schmitz A, Mevissen M, Thormann W, Enantioselective capillary electrophoresis for identification and characterization of human cytochrome P450 enzymes which metabolize ketamine and norketamine in vitro. Journal of Chromatography A 1217 7942–7948 (2010) [PubMed: 20609441]
43. Duncan GE, Moy SS, Knapp DJ, Mueller RA, Breese GR, Metabolic mapping of the rat brain after subanesthetic doses of ketamine: potential relevance to schizophrenia. Brain Res 787, 181–190 (1998). [PubMed: 9518601]
44. Miyamoto S, Leipzig JN, Lieberman JA, Duncan GE, Effects of ketamine MK-801, and amphetamine on regional brain 2-deoxyglucose uptake in freely moving mice. Neuropsychopharmacology 22, 400–412 (2000). [PubMed: 10700659]
45. Murray EA, Rudebeck PH. Specializations for reward-guided decision-making in the primate ventral prefrontal cortex Nat Rev Neurosci. 19, 404–417 (2018) [PubMed: 29795133]
46. Hare BD, Duman RS, Prefrontal cortex circuits in depression and anxiety: contribution of discrete neuronal populations and target regions. Mol Psychiatry, (2020).
47. Klein ME, Chandra J, Sheriff S, and Malinow R, Opioid system is necessary but not sufficient for antidepressive actions of ketamine in rodents. PNAS 117. 2656–2662 (2020) [PubMed: 31941713]
48. Jacobson ML, Simmons SC, Wulf HA, Cheng H, Feng Y, Feresteh, et al. , Protracted Effects of Ketamine Require Immediate Kappa Opioid Receptor Activation and Long-Lasting Desensitization. The FASEB Journal, 34, (S1) (2020)
49. Williams NR, Heifets BD, Blasey C, Sudheimer K, Pannu J, Pankow H et al. , Attenuation of antidepressant effects of ketamine by opioid receptor antagonism. Am. J. Psychiatry 175, 1205–1215 (2018) [PubMed: 30153752]

50. Williams NR, Heifets BD, Bentzley BS, Blasey C, Sudheimer KD, Hawkins J et al. , Attenuation of antidepressant and antisuicidal effects of ketamine by opioid receptor antagonism. Mol. Psychiatry 24, 1779–1786 (2019) [PubMed: 31467392]
51. Milligan G, Principles: extending the utility of [35S]GTP gamma S binding assays. Trends Pharmacol Sci 24, 87–90 (2003). [PubMed: 12559773]
52. Vogt LJ, Sim-Selley LJ, Childers SR, Wiley RG, Vogt BA, Colocalization of mu-opioid receptors and activated G-proteins in rat cingulate cortex. J Pharmacol Exp Ther 299, 840–848 (2001). [PubMed: 11714867]
53. Tejeda HA, Counotte DS, Oh E, Ramamoorthy S, Schultz-Kuszak KN, Bäckmanet al CM, Prefrontal cortical kappa-opioid receptor modulation of local neurotransmission and conditioned place aversion. Neuropsychopharmacology 38, 1770–1779 (2013) [PubMed: 23542927]
54. Kalivas PW, Neurotransmitter regulation of dopamine neurons in the ventral tegmental area. Brain Res Brain Res Rev 18, 75–113 (1993). [PubMed: 8096779]
55. R.A. Wise and P.P. Rompre Brain dopamine and reward. Annu Rev Psychol 40, 191–225 (1989) [PubMed: 2648975]
56. Johnson SW and North RA Opioids excite dopamine neurons by hyperpolarization of local interneurons. J Neurosci 12, 483–488 (1992) [PubMed: 1346804]
57. Margolis EB, Lock H, Chefer VI, Shippenberg TS, Hjelmstad GO, Fields HL, κ opioids selectively control dopaminergic neurons projecting to the prefrontal cortex. PNAS 103, 2938–2942 (2006) [PubMed: 16477003]
58. Badiani A, Belin D, Epstein D, Calu D and Shaham Y. Opiate versus psychostimulant addiction: the differences do matter. Nat Rev Neurosci 12, 685–700. (2011) [PubMed: 21971065]
59. Hashimoto K, Kakiuchi T, Ohba H, Nishiyama S, Tsukada H, Reduction of dopamine D2/3 receptor binding in the striatum after a single administration of esketamine, but not R-ketamine: a PET study in conscious monkeys. European Archives of Psychiatry and Clinical Neuroscience 267, 173–176 (2017) [PubMed: 27091456]
60. Slifstein M, Kegeles LS, Xu X, Thompson JL, Urban N, Castrillon J, et al. , Striatal and extrastriatal dopamine release measured with PET and [18F]fallypride. Synapse 64, 350–362 (2011)
61. McDougall SA, Moran AE, Baum TJ, Apodaca MG, Real V, Effects of ketamine on the unconditioned and conditioned locomotor activity of preadolescent and adolescent rats: impact of age, sex, and drug dose. Psychopharmacology 234, 2683–2696 (2017) [PubMed: 28589265]
62. Mucha RF, van der Kooy D D, O'Shaughnessy M and Bucenieks P, Drug reinforcement studied by the use of place conditioning in rat. Brain Res 243, 91–105. (1982) [PubMed: 6288174]
63. Yokel RF, Intravenous self-administration: Response rates, the effects of pharmacological challenges, and drug preference, in Methods of assessing the reinforcing properties of abused drugs (Bozarth MA ed) pp 1–34, Springer-Verlag, New York. (1987)
64. Richardson NR, Roberts DC, Progressive ratio schedules in drug self-administration studies in rats: a method to evaluate reinforcing efficacy. J Neurosci Methods 66, 1–11 (1996) [PubMed: 8794935]
65. Venniro M, Banks ML, Heilig M, Epstein DH, Shaham Y, Improving translation of animal models of addiction and relapse by reverse translation. Nat rev Neurosci Brain Res 21, 625–623 (2020)
66. Matsumoto RR, Nguyen L, Kaushal N, Robson MJ, Sigma (σ) receptors as potential therapeutic targets to mitigate psychostimulant effects, Adv Pharmacol. 69, 323–86 (2014) [PubMed: 24484982]
67. Kalivas PW and Stewart J, Dopamine transmission in the initiation and expression of drug- and stress-induced sensitization of motor activity. Brain Res Rev 16, 223–244. (1991) [PubMed: 1665095]
68. Tan Y and Hashimoto K, Risk of psychosis after repeated intermittent administration of (S)-ketamine, but not (R)-ketamine, in mice. Journal of Affective Disorders 269, 198–200 (2020) [PubMed: 32339136]
69. Chang L, Zhang K, Pu Y, Qu Y, Wang S, Xiong Z, et al. , Comparison of antidepressant and side effects in mice after intranasal administration of (R,S)-ketamine, (R)-ketamine, and (S)-ketamine. Pharmacology biochemistry and Behavior 181, 53–59 (2019)

70. O'Brien CP, Childress AR, McLellan AT and Ehrman R Classical conditioning in drug-dependent humans. Ann N Y Acad Sci 654, 400–415 (1992) [PubMed: 1632593]
71. Zanos P, Highland JN, Liu X, Troppoli TA, Georgiou P, Lovett J, et al. , (R)-Ketamine exerts antidepressant actions partly via conversion to (2R,6R)-hydroxynorketamine, while causing adverse effects at sub-anaesthetic doses. Br J Pharmacol 176, 2573–2592 (2019) [PubMed: 30941749]
72. Yang Y, Cui Y, Sang K, Dong Y, Ni Z, Ma S, et al. , Ketamine blocks bursting in the lateral habenula to rapidly relieve depression. Nature 14, 317–322 (2018)
73. Zhang K, Hashimoto K, An update on ketamine and its two enantiomers as rapid-acting antidepressants. Expert Review of Neurotherapeutics 19, 83–92 (2018) [PubMed: 30513009]
74. Nair AB, Jacob S A simple practice guide for dose conversion between animals and human. J Basic Clin Pharm. 7, 27–31 (2016) [PubMed: 27057123]
75. Morris ED, Yoder KK, Positron emission tomography displacement sensitivity: predicting binding potential change for positron emission tomography tracers based on their kinetic characteristics. J Cereb Blood Flow Metab 27, 606–617 (2007) [PubMed: 16788713]
76. US Food and Drug Administration, Joint Meeting of the Psychopharmacologic Drugs Advisory Committee and the Drug Safety and Risk Management Advisory Committee.https://www.fda.gov/advisory-committees/february-12-2019-joint-meeting-psychopharmacologic-drugs-advisory-committee-pdac-and-drug-safety-and#event-materials February 12, 2019
77. Witkin JM, Kranzler J, Kaniecki K, Popik P, Smith JL, Hashimoto K, et al. , R-(−)-ketamine modifies behavioral effects of morphine predicting efficacy as a novel therapy for opioid use disorder, Pharmacol Biochem Behav. 194, 172927 (2020) [PubMed: 32333922]
78. Yoon G, Petrakis IL, Krystal JH, Association of combined naltrexone and ketamine with depressive symptoms in a case series of patients with depression and alcohol use disorder. JAMA Psychiatry 76, 337–338 (2019) [PubMed: 30624551]
79. Heifets BD, Williams NR, Bentzley BS, Schatzberg AF, Rigorous Trial Design Is Essential to Understand the Role of Opioid Receptors in Ketamine's Antidepressant Effect. JAMA Psychiatry 76, 657–659 (2019) [PubMed: 31042274]
80. F Pacheco D, Romero T, Duarte I, Central antinociception induced by ketamine is mediated by endogenous opioids and μ- and δ-opioid receptors. Brain research 1562, 69–75 (2014) [PubMed: 24675031]
81. Vollenweider FX, Leenders KL, Oye I, Hell D, Angst J, Differential psychopathology and patterns of cerebral glucose utilisation produced by (S)- and (R)-ketamine in healthy volunteers using positron emission tomography (PET). Eur Neuropsychopharmacol 7, 25–38 (1997). [PubMed: 9088882]
82. Carlson PJ, Diazgranados N, Nugent AC, Ibrahim L, Luckenbaugh DA, Brutsche N et al. , Neural correlates of rapid antidepressant response to ketamine in treatment-resistant unipolar depression: a preliminary positron emission tomography study. Biol Psychiatry. 15, 1213–21 (2013)
83. Masaki Y, Kashiwagi Yuto, Watabe Hiroshi, Abe Kohji, (R)- and (S)-ketamine induce differential fMRI responses in conscious rats. Synapse 73, e22126 (2019) [PubMed: 31397936]
84. N-S, Quiroz C, Bonaventura J, Bonifazi A, Cole TO, Purks J, Opioid–galanin receptor heteromers mediate the dopaminergic effects of opioids. J Clin Invest 129, 2730–2744 (2019) [PubMed: 30913037]
85. Bonaventura J Eldridge MAG, Hu F, Gomez JL, Sanchez-Soto M, Abramyan A, et al. , High-potency ligands for DREADD imaging and activation in rodents and monkeys. Nat Commun 10, 4627 (2019) [PubMed: 31604917]
86. Fredriksson I I, Applebey SV, Minier-Toribio A, Shekara A A, Bosser JM and Shaham Y Y, Effect of the dopamine stabilizer (−)-OSU6162 on potentiated incubation of opioid craving after electric barrier-induced voluntary abstinence. Neuropsychopharmacology 45, 770–779. (2020) [PubMed: 31905372]

Significance statement

Our results provide evidence suggesting that the abuse liability of racemic ketamine in humans is primarily due to the pharmacological effects of (S)-ketamine but not (R)-ketamine. These preclinical results have implications for the use of ketamine enantiomers for the treatment of depression.

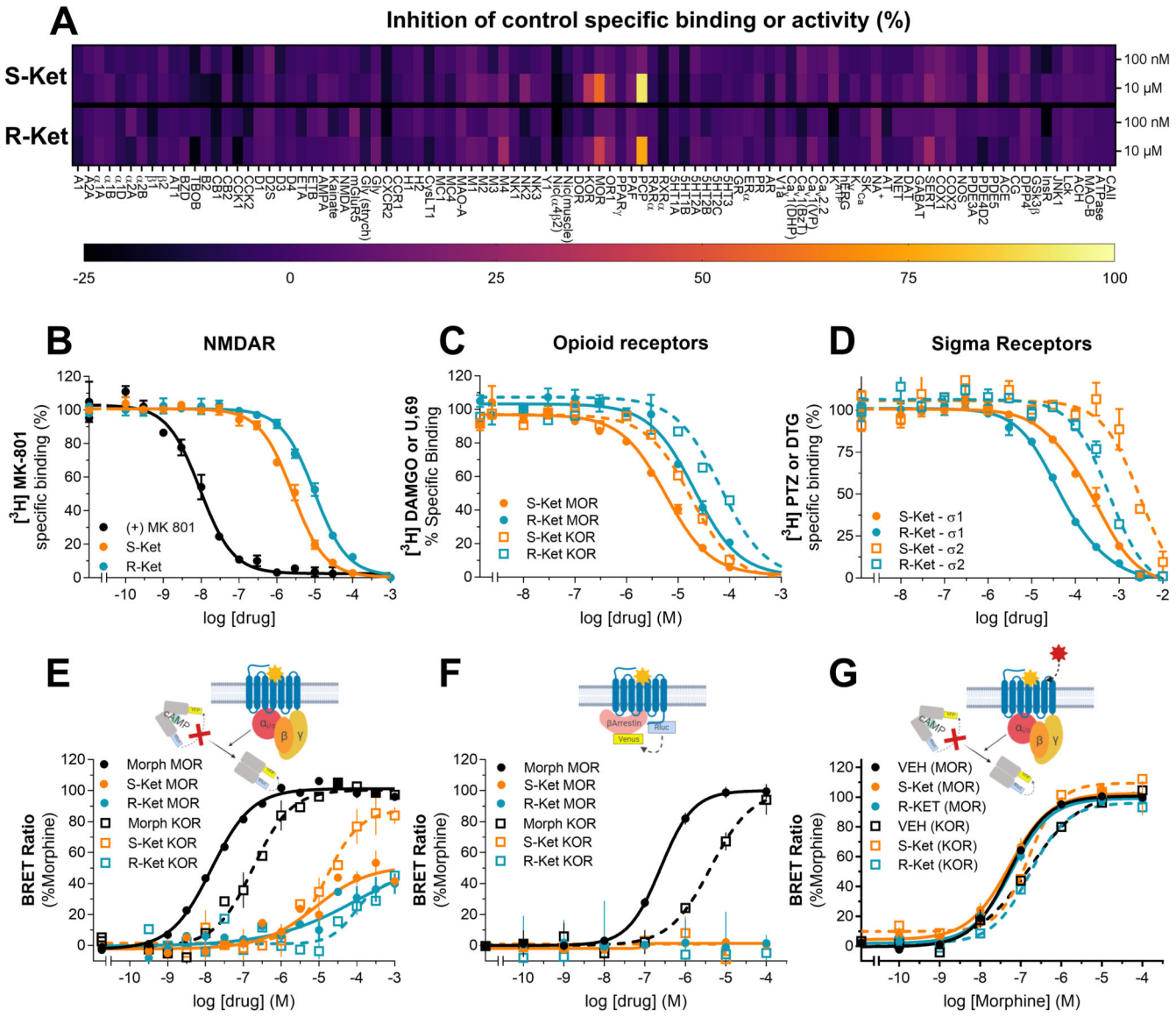

Figure 1. Divergent pharmacodynamics of ketamine enantiomers.

Receptor and enzyme competitive screen at two concentrations (100 nM and 10 µM) of S- and (R)-ketamine (**A**). Competition binding assays of (S)-ketamine (orange) or (R)-ketamine (blue) enantiomers versus radioligands labeling NMDA receptors (**B**), opioid receptors (**C**): MOR (solid circles) and KOR receptors (open squares) or sigma receptors (**D**): Sigma-1 (solid circles) and Sigma-2 (open squares) receptors. All binding assays were performed in rat whole brain (except cerebellum) membrane suspensions. *In vitro* signaling elicited by morphine or ketamine enantiomers in HEK-293 cells transiently transfected with MOR or KOR (**E-G**): ketamine enantiomers activate the G-protein (**E**) but not ß-arrestin signaling (**F**), and do not inhibit morphine G-protein signaling (**G**). All data points are mean ± SEM of representative experiments performed in triplicate (experiments were performed 3 to 6 times to estimate the parameters (K_i, EC_{50} and E_{max}) reported in the main text.

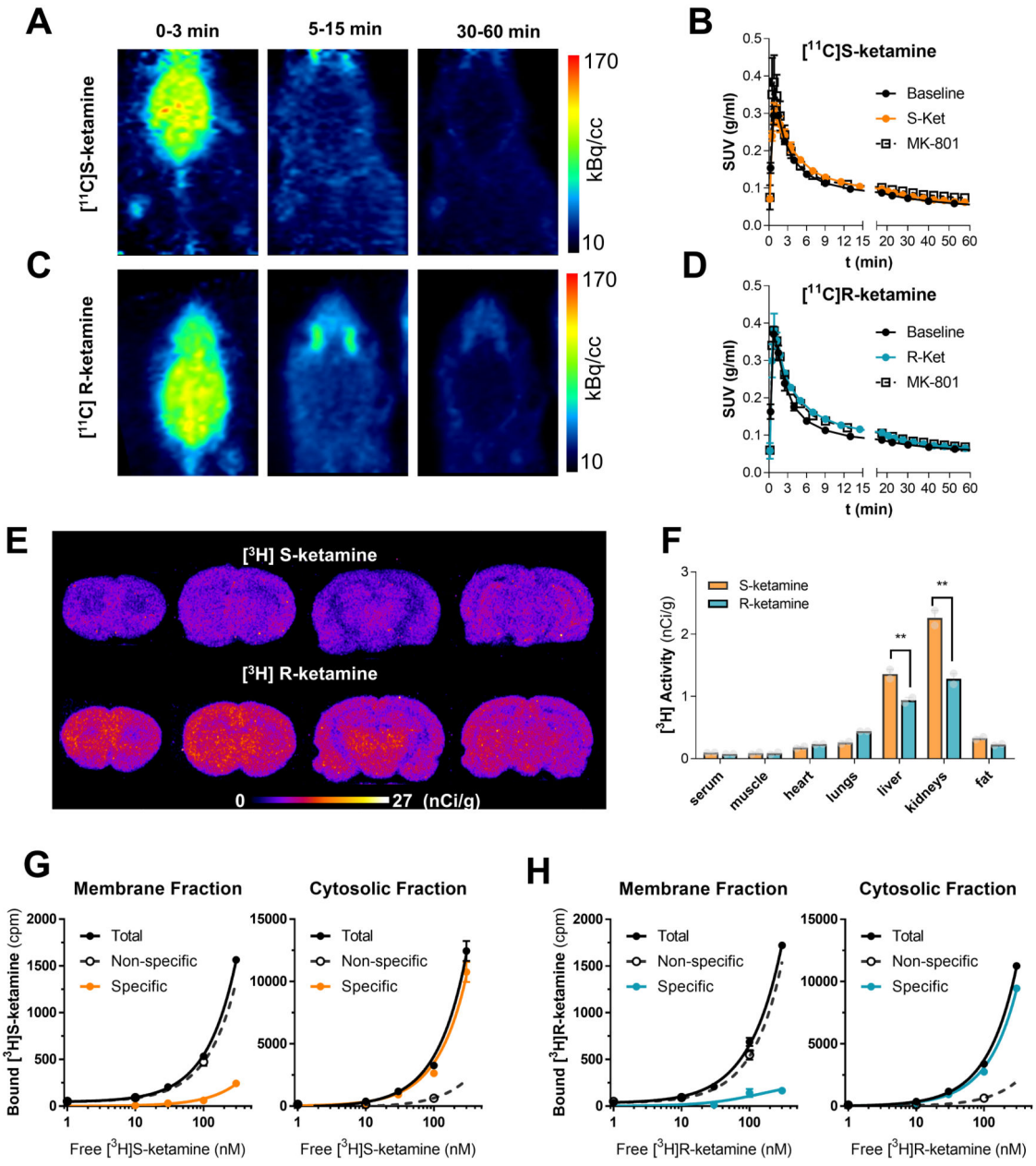

Figure 2. Rapid brain uptake, fast clearance and no high affinity target for ketamine enantiomers.

Representative PET images obtained after bolus IV administration of [^{11}C](S)-ketamine (**A**) or [^{11}C](R)-ketamine (**C**) at different time windows. After the initial brain uptake, activity remains exclusively in the harderian glands (nonspecific accumulation). In **B** and **D**, whole brain time activity curves measured after a bolus administration of either [^{11}C]-ketamine enantiomer preceded by a pretreatment with the cold enantiomer (10 mg/kg IP) or the NMDAR non-competitive antagonists (+)-MK-801 (0.1mg/kg, IP). Data points are mean ±

SD of standardized uptake values (SUV, g/ml) obtained from at least two PET images per condition. In **E**, representative autoradiograms of coronal brain sections of rats injected (IV, 1μCi/g) with radiolabeled [^{3}H](S)-ketamine and [^{3}H](R)-ketamine and euthanized at 40 min post injection. In **F**, biodistribution of [^{3}H](S)-ketamine and [^{3}H](R)-ketamine 40 min after IV administration. Saturation binding experiments using membrane and cytosolic fractions of rat brain homogenates indicate the lack of a high affinity specific binding (displaceable and saturable) (**G-H**).

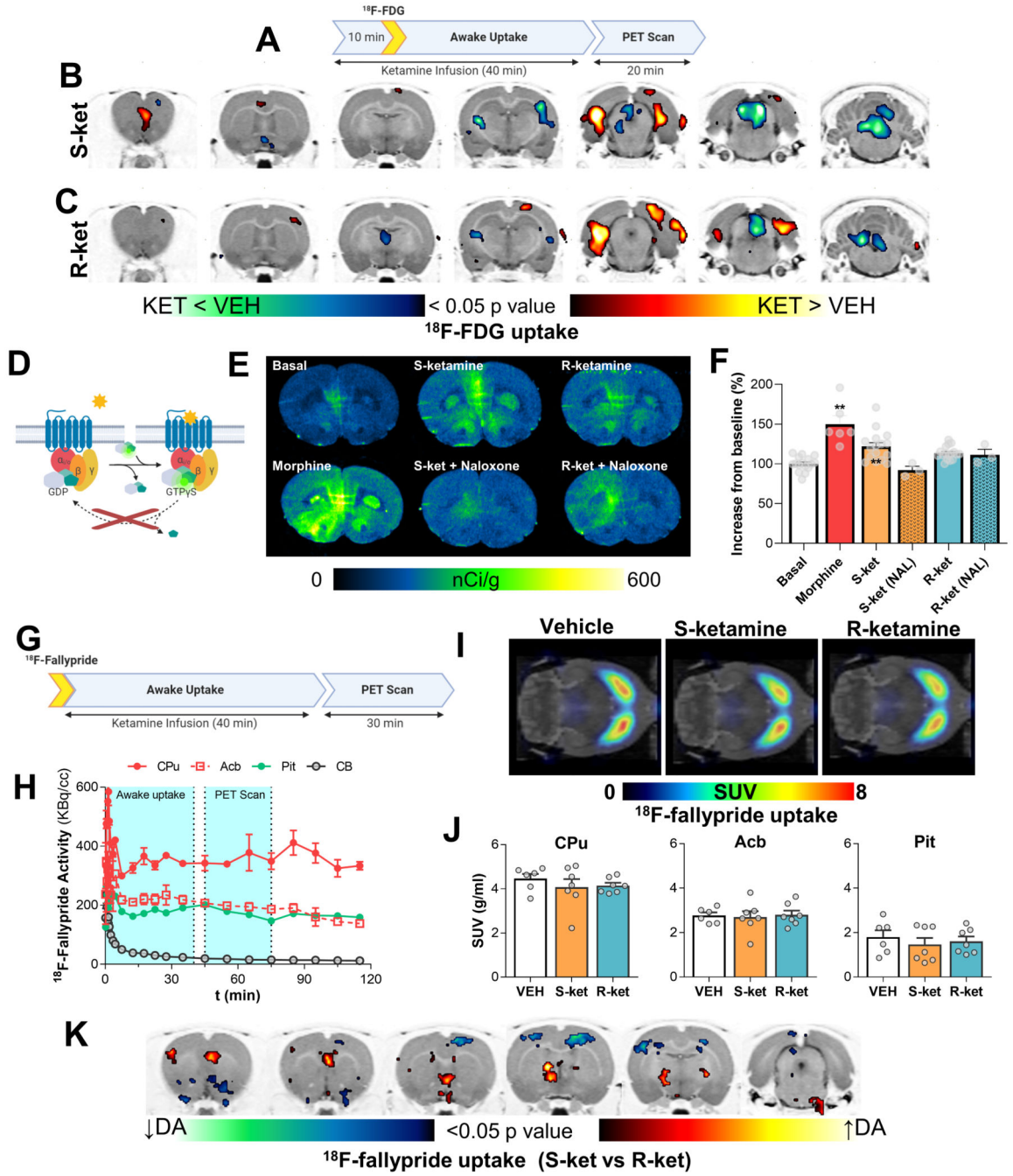

Figure 3. Functional brain imaging reveals regional differences in the effects of ketamine enantiomers.

A to **C**, (S)- or (R)-ketamine infusions (15mg/kg/h) have differential effects on metabolic activity evaluated as accumulation and trapping of [^{18}F]FDG in the brains of awake, freely-moving rats. The rats were anesthetized and scanned 40 min after drugs and [^{18}F]FDG (decay half-life =~110 min) were administered, providing a “snapshot” of metabolic activity during the awake, freely-moving state. Brain-wide voxel-based analysis was used to evaluate differences on activity using a one-way ANOVA. Color shaded areas in **B**

and **C** represent clusters of voxels (≥100) with significant ($p<0.05$) increases or decreases in metabolic rate compared to saline infusions. **D** to **F**, G-protein signaling induced by ketamine enantiomers in the PFC indicates MOR-mediated signaling by (S)-ketamine. **G** to **K**, changes in dopamine tone elicited by infusion of the ketamine enantiomers evaluated as [^{18}F]-Fallypride (dopamine D2 antagonist) uptake in awake freely moving animals (**G**). After ketamine and [^{18}F]fallypride animals were anesthetized and a static PET image was acquired for 30 minutes (**G**). PET images (**I-J**) were analyzed using both region of interest-wise and voxel-wise analysis methods. In **K**, shaded areas represent clusters of voxels (≥100) with significant ($p<0.05$) increases or decreases in dopamine tone between (S)- and (R)-ketamine. Abbreviations: CPu, Caudate-Putamen; Acb, Nucleus Accumbens; Pit, Pituitary gland.

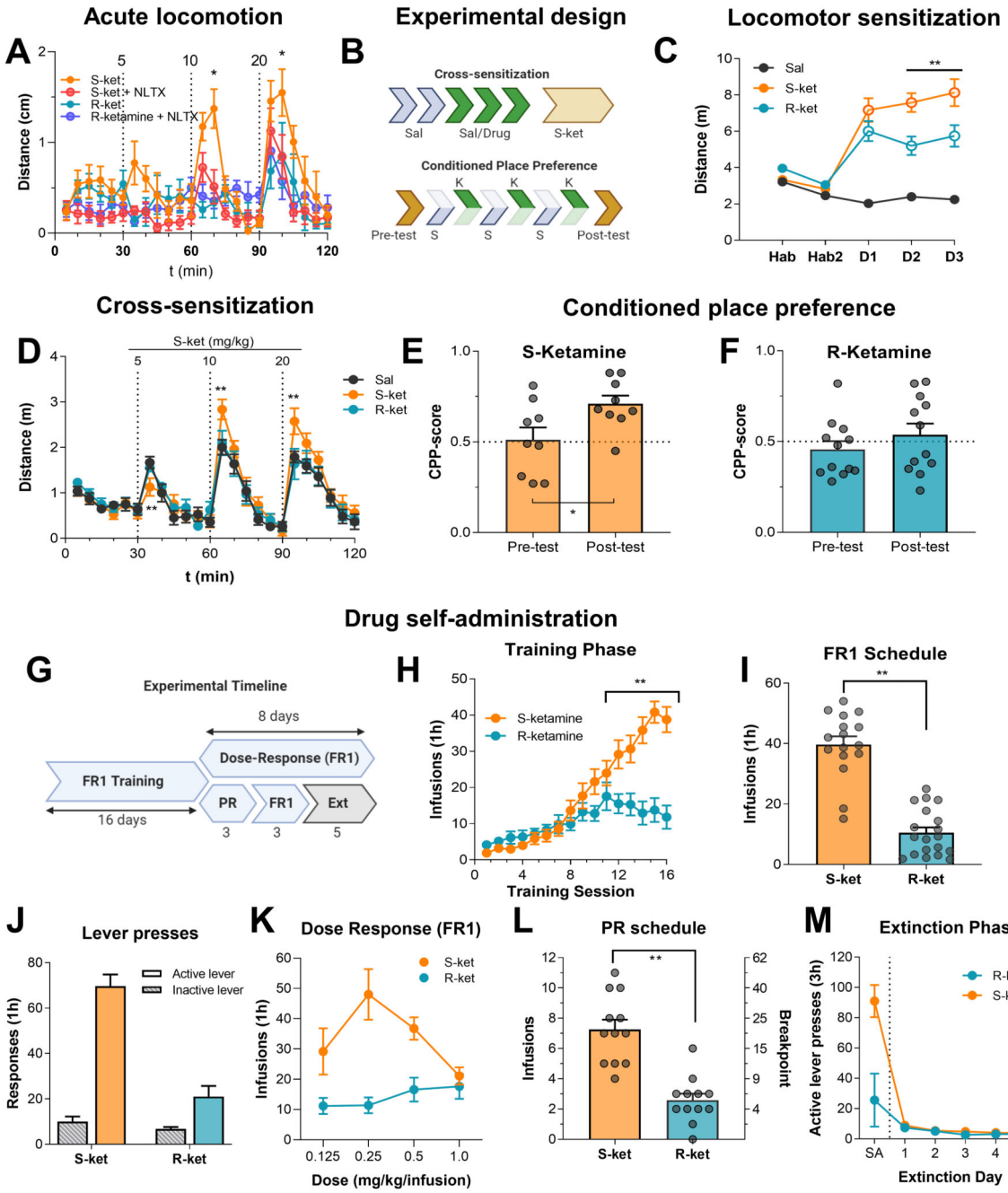

Figure 4. Behavioral effects of ketamine enantiomers: locomotor activity, conditioned place preference, and drug self-administration.

(A) Acute locomotor activity: Male mice were placed in an open field arena and injected with saline and increasing doses of (S)-ketamine or (R)-ketamine (5, 10 and 20 mg/kg, IP) every 30 min, with or without pretreatment (10 min) with naltrexone (10 mg/kg, IP). Plots display distance traveled in open field arenas for in 5 min time bins, * denote statistical significance ($p<0.05$) between (S)-ketamine and (S)-ketamine with naltrexone pretreatment. **(B-D)** Locomotor sensitization after repeated injections: Male mice were

habituated to the arenas for two days (Hab1–2) and then injected with vehicle (saline, black), (S)-ketamine (20 mg/kg, orange), (R)-ketamine (20 mg/kg, blue) for three days (D1–3). On day 8, the mice received increasing doses of (S)-ketamine (5, 10 and 20 mg/kg). Plots display distance traveled in open field arenas for 30 min after each drug. ** denote statistical significance ($p<0.01$) between (S-) and (R)-ketamine groups. **(E-F)** CPP: Male mice were injected with one of the ketamine enantiomers (10 mg/kg) or saline on either side of the CPP arena for 6 days and were allowed to explore both sides at the end of the conditioning phase. The preference for the drug-paired side was quantified as a CPP score. Data points are displayed as mean ± SD of 12 mice per condition or individual data points. * denotes statistical significance ($p<0.05$) from the pre-test condition. **(G-M)** Self-administration and extinction: **(G)** Experimental timeline for self-administration and extinction in male and female rats. **(H-J)** Ketamine self-administration training: mean±SEM number of infusions and active and inactive lever presses under the FR1 20-s timeout reinforcement schedule. **(K)** Dose response curve: mean±SEM number of infusions for different unit doses of the two enantiomers under the FR1 20-s timeout reinforcement schedule. **(L)** Progressive ratio: mean±SEM number of infusions and breakpoint (final ratio completed) for (S)-ketamine and (R)-ketamine under the progressive ratio reinforcement schedule. **(M)** Extinction responding: mean±SEM number of active lever presses during the last retraining session under the FR1 20-s timeout reinforcement schedule (denoted as SA) and during the subsequent extinction session. During the extinction session, lever presses led to contingent presentations of the discrete cue previously paired with (S)-ketamine and (R)-ketamine self-administration training and retraining, but not drug infusions**: significant difference ($p < 0.01$) between groups. Abbreviations: SA, self-administration; Ext, extinction, (S)-ketamine, (S)-ket; (R)-ketamine, (R)-ket; FR1, fixed ratio 1; NLTX, naltrexone.